

Award Accounts

The Chemical Society of Japan Award for Young Chemists for 2002

Ab Initio Extended Density Functional Theory for Strongly Correlated Electron Systems: Fundamental Aspects of the Broken-Symmetry Approach and Possible Applications for Molecular Material Design

Shusuke Yamanaka* and Kizashi Yamaguchi

Department of Chemistry, Graduate School of Science, Osaka University, Machikaneyama, Toyonaka 560-0043

Received October 24, 2003; E-mail: syama@chem.sci.osaka-u.ac.jp

We review the extended density functional theory (DFT), in which we make full use of the broken-symmetry feature of the Kohn–Sham (KS) DFT. The theory is based on the classification of broken-symmetry solutions of the Hartree–Fock theory, which has been developed by some precursors in the field “broken-symmetry quantum chemistry”. We describe the fundamental characteristics of the DFT based on generalized spin orbitals (GSOs) in relation to the extension of the constrained search region of DFT. In addition, some important applications, such as noncollinear magnetism of multicenter radicals and radical dissociation followed by spin rotations that are firstly enabled by the use of the GSO-DFT, are presented. Furthermore, future directions covering quantum fluctuations between several collective modes, ab initio molecular dynamics, and relativistic phenomena are also described from the viewpoint of search regions of the extended DFT.

In solid state physics, the transition metal ions play essential role for electronic properties such as magnetism and conductivity of materials.¹ The guideline to design functionality is devotedly to control (i) the orbital-filling of metal sites and (ii) the geometry and the constant of the lattice. On the other hand, during the past three decades, there has been remarkable progress in the field “molecular-based material science”, in which ones can utilize more flexible electronic characteristics of carriers (molecules) by exploring substituent effects and pliable lattices. Indeed, the various compounds such as the organic ferromagnetic materials,² charge-transfer complex,³ organic superconductors,⁴ etc., have been synthesized. In order to investigate these systems, we should first note that the electron correlation plays a crucial role in determining such electronic properties of materials. In particular, the various magnetic behaviors of strongly correlated systems originate essentially from the electron correlation due to the coulomb repulsion terms in the Hamiltonian. The second important point is that the molecular orbital theory plays a important role to describe the intra and intermolecular interactions. The electronic structure theories in the first generation are empirical ones using parameters to understand the essential feature of the target materials.⁵ As computational environments have been improved, theoretical efforts to predict experimental physical and chemical properties of materials, the so-called ab initio approach for material design, have drastically increased.⁶ In the field of molecular magnetism, the situation has enabled us to compute a priori the value of the effective exchange interaction that determines the basic features of molecular magnetic systems.²

There are various approaches that are called “ab initio” methods; they differ in on basis sets, boundary conditions, and/or theoretical backgrounds. The most significant branch is based on fundamental variables. The electron correlation is originally a quantum phenomenon as described below, so that the use of wavefunctions is reasonable. Indeed, in the field of quantum chemistry, multi-reference (MR) wavefunction theories (WFT) such as configuration interaction (CI) and coupled-cluster (CC) methods⁶ are successfully applied for small molecules, even in their excited states. However, the expansion of a wavefunction becomes a bottleneck when one computes macromolecules such as bioenzymes or functional materials. In the 1990s, instead of WFT, the Kohn–Sham (KS) density functional theory (DFT) has been brought to light.⁷ The fundamental variable here is a density or a spin-density. The KS-DFT had been explored mainly in the field of solid state physics before the 1980s, but nowadays it has become the most popular method in the quantum chemistry. One merit of the KS-DFT is that it can include the electron correlation effects without wavefunction expansion, which enables us to compute more huge systems than those we can do by WFT. In addition, the trend of computational resources for the computational science has helped KS-DFT to become widespread. Since the middle of the 1990s, a parallel computational environment utilizing the high-performance personal computers⁸ with the message-passing interface (MPI) library⁹ has become a main facility, supplanting supercomputers and workstations. The explosive evolution of the computation technique is now going into the so-called “Grid computing”, in which the computational resour-

ces are far from each other, but are connected by the broadband network.¹⁰ This direction is expected to be a main stream of computational chemistry-and-physics in this 21-th century towards the material design. The computations employing DFT exhibit, in principle, linear scaling with respect to the size of the system,¹¹ to determine the ground state electronic structure of molecular compounds, so they are suited for such computational environments.

Despite such promising aspects, the KS-DFT has some problems. For instance, the symmetry of solutions is broken in a simple homolysis of a chemical bond; the origin of this problem is discussed in this paper. This feature is thought to be a positive aspect of broken-symmetry (BS) KS-DFT to describe the molecular magnetism as in the case of the Hartree–Fock theory.^{2,6} We further exploited the applicability of BS KS-DFT for more complicated situations by choosing a broken-symmetry pattern deliberately, as presented below. In the context of a fundamental theory of KS-DFT, the broken-symmetry implies the extension of the DFT search region.

Thus, in this paper, we review ab initio approaches of the extended DFT as well as those of WFT; these were utilized for predicting intra-and-intermolecular magnetic interactions of molecular magnetic systems. As a preliminary, we describe the theoretical background of Hartree–Fock (HF) approximation that is directly related with the KS-DFT in many theoretical points. Since our focus is on the spin broken-symmetry approaches and these applications, most of our formulations are developed in a fully spin-unrestricted manner with generalized spin orbitals (GSOs), which are usually neglected in many instructive reviews and texts.^{6,7} There are two roles of broken-symmetry of GSO solutions. The first role is for the description of physical properties which can be represented by using the first order reduced density matrix. As a fundamental theory to explain this point, we describe the classification of generalized HF (GHF) solutions, which is a guideline of GSO computations. Another role is for the electron correlation, which is missed by restricted HF solutions in the case of the strongly correlated systems. Next, we discuss the complete-active-space (CAS) based methods as traditional WFT's. The facility and power of these approaches are discussed in relation to applications of molecular magnetic systems, as well as the promising computational direction of WFT's.

First, the GSO version of the DFT formulation will be described. We shall offer a very simple but significant example against a statement that KS theory could become an exact theory in general. From this discussion, we will see the reason that the broken-symmetry KS-DFT⁷ theory works well for strongly correlated systems, as well as the limitation of the symmetry-adapted KS theory. A most important point of GSO-DFT is its applicability to various classes of molecular magnetism. So, we discuss the relationship between the constrained search region of spin density matrices and the spin-rotational and time-reversal symmetry as a theoretical basis of GSO-DFT following a similar method to that of the GHF theory.

To present the potentials of the GSO-DFT method, we examine some examples of non-collinear molecular magnetic systems on which the GSO treatment is essential for the description of the ground-state spin structure. The major feature of our recent researches is exploring the new applicability of

DFT for some non-collinear molecular magnetism phenomena. For instance, the three-dimensional spin structure of tetrahedral magnetic clusters and the bond-cleavage of oxygen-type molecule have never been treated by any usual DFT computation. The computational results are discussed in relation to spin-degenerate and spin-frustrated features of the classical spin-vector model.

At the end of this paper, some future directions in line with the extended DFT are discussed. First, the inevitable defects of GSO-DFT and a post GSO-DFT approach are also discussed. The remedy for them is not based on an usual complete-active-space (CAS) based WFT approach, but on the resonation of GSO-DFT solutions. Next, towards the new implementation of quantum mechanics/molecular mechanics (QM/MM),¹² a scheme to partition macromolecular systems into functional units is proposed, in which the classification of GSO solutions is fully explored to treat the QM region. Finally, we describe the relativistic extension for the quantum electrodynamics (QED) framework and its relation with the GSO-DFT approach. The relativistic extension not only provides a comprehensive theory of extended DFT, but also is essential to treat new physics such as superconductivity induced by spin-fluctuations of heavy fermions, in which both relativistic effects and the strong electron correlation between f orbitals play important roles.

Electron Correlation and an Exact and Straightforward Electronic Structure Theory

In quantum chemistry, the traditional way to treat the electron correlation is based on a many electron wavefunction⁶

$$\langle \mathbf{x}_1, \mathbf{x}_2, \dots, \mathbf{x}_N | \Psi \rangle = \Psi(\mathbf{x}_1, \mathbf{x}_2, \dots, \mathbf{x}_N). \quad (1)$$

Here, \mathbf{x}_i denotes both a spatial coordinate (\mathbf{r}_i) and a spin coordinate (s_i) for the i -th electron. With the WFT, it is reasonable to use the electronic structure theory because the electron interactions except the classical coulomb interaction between the density distributions are essentially quantum mechanical phenomena. Electron correlation interactions can be divided into the exchange and the correlation interactions. The former is due to the Pauli principle that forbids two electrons with parallel spins from occupying the same position. This principle imposes the antisymmetric condition on a wavefunction, for instance of an N electron system,

$$\Psi(\mathbf{x}_1, \dots, \mathbf{x}_i, \dots, \mathbf{x}_j, \dots, \mathbf{x}_N) = -\Psi(\mathbf{x}_1, \dots, \mathbf{x}_j, \dots, \mathbf{x}_i, \dots, \mathbf{x}_N). \quad (2)$$

In order to obtain the most stable electronic structure, according to the Rayleigh–Ritz minimal principle, the minimization procedure,

$$E_0 = \text{Min}_\Psi \langle \Psi | \hat{H} | \Psi \rangle \quad (3)$$

for the ab initio Hamiltonian,

$$\begin{aligned} \hat{H} &= \sum_{i=1}^N \left(\frac{-\nabla_i^2}{2} + \sum_{j=1}^{N_{\text{atoms}}} v_{N_{je}}(\mathbf{x}_i) \right) + \sum_{i < j}^N \frac{1}{|\mathbf{r}_i - \mathbf{r}_j|} \\ &= \sum_{i=1}^N h_i^{\text{core}} + \sum_{i < j}^N \frac{1}{|\mathbf{r}_i - \mathbf{r}_j|} \end{aligned} \quad (4)$$

should be conducted. Here the Ψ in the search region is any N electron wavefunction satisfying the normalized condition and the antisymmetric condition given by Eq. 2. We combined the kinetic term $-\nabla_i^2/2$ and the nuclear attraction term $v_{Nje}(\mathbf{x}_i)$ into the core Hamiltonian term h_i^{core} at the right side of Eq. 4. We here note that the electron correlation arises from the quantum effect due to the non-commutative relation:

$$\left[\sum_{i=1}^N h_i^{\text{core}}, \sum_{i<j}^N \frac{1}{|\mathbf{r}_i - \mathbf{r}_j|} \right] \neq 0. \quad (5)$$

This relation causes both some difficulties of the electron correlation problem as well as some fruitful phenomena connected to the quantum many body effects. For this non-commutative relation, the $3N$ dimensional minimization problem, Eq. 3, can not be divided into N one-particle problems.

The minimization over the functional space consisting of $3N$ dimensional wavefunctions can be implemented in principle. Indeed we developed the electron wavepacket (EWP) approach¹³ as a straightforward method to solve Eq. 3, in which the antisymmetrized real space basis and the stimulated annealing scheme are employed to obtain the exact solutions. The EWP is instructive to understand the electron correlation problem, but is not a practical tool since it consumes huge computational costs. For instance, if we use 1000^3 grids to express the three-dimensional real space, 16×1000^6 bytes = 16 TB is needed as a computational memory to obtain the exact EWP solution of a hydrogen molecule. Thus, the linear combination of atomic orbitals (LCAO) method, which is introduced by Roothaan¹⁴ and is usually started from the Hartree–Fock approximation, is essential for the actual implementation of quantum chemistry.

Generalized Hartree–Fock Approximation and Its Origin of Symmetry-Breaking

In the Hartree–Fock (HF) approximation, which is the standard starting point of the ab initio LCAO theories,^{6,14} we employ the Slater determinant:

$$\begin{aligned} \Phi(\mathbf{x}_1, \mathbf{x}_2, \dots, \mathbf{x}_N) &= \langle \mathbf{x}_1, \mathbf{x}_2, \dots, \mathbf{x}_N | \psi_1, \psi_2, \dots, \psi_N \rangle \\ &= (N!)^{-1/2} \begin{vmatrix} \psi_1(\mathbf{x}_1) & \psi_2(\mathbf{x}_1) & \cdots & \psi_N(\mathbf{x}_1) \\ \psi_1(\mathbf{x}_2) & \psi_2(\mathbf{x}_2) & \cdots & \psi_N(\mathbf{x}_2) \\ \vdots & \vdots & & \vdots \\ \psi_1(\mathbf{x}_N) & \psi_2(\mathbf{x}_N) & \cdots & \psi_N(\mathbf{x}_N) \end{vmatrix}, \end{aligned} \quad (6)$$

as a trial function for the minimization procedure in Eq. 3. Here ψ_i is a trial molecular orbital (MO) for i -th electron. By applying Lagrange multipliers method, one obtains the HF equations, which are coupled to each other via electron correlation terms:

$$\left\{ h_i^{\text{core}} + \sum_j (J_j(\mathbf{r}_1 s_1) - K_j(\mathbf{r}_1 s_1)) \right\} \psi_i(\mathbf{r}_1 s_1) = \varepsilon_i \psi_i(\mathbf{r}_1 s_1). \quad (7a)$$

Here, J_j and K_j are coulomb and exchange operators defined by:

$$J_j(\mathbf{r}_1 s_1) \psi_i(\mathbf{r}_1 s_1) = \int d\mathbf{r}_2 \frac{\psi_j^*(\mathbf{r}_2 s_1) \psi_j(\mathbf{r}_2 s_1)}{|\mathbf{r}_1 - \mathbf{r}_2|} \psi_i(\mathbf{r}_1 s_1), \quad (8a)$$

$$K_j(\mathbf{r}_1 s_1) \psi_i(\mathbf{r}_1 s_1) = \sum_{s_2} \int d\mathbf{r}_2 \frac{\psi_j^*(\mathbf{r}_2 s_2)}{|\mathbf{r}_1 - \mathbf{r}_2|} P_{12} \psi_j(\mathbf{r}_2 s_2) \psi_i(\mathbf{r}_1 s_1), \quad (8b)$$

respectively. The operator in the brace at the left side of Eq. 7 is denoted as the Fock operator. We here note that the exchange operator defined by Eq. 8b includes the permutation of spin variables together with spatial coordinates, leading to coupled equations among different spin orbitals, as

$$\begin{aligned} &\sum_{s_2} \left[\delta_{s_1 s_2} \left\{ h_i^{\text{core}} + \sum_j J_j(\mathbf{r}_1 s_1) \right\} \psi_i(\mathbf{r}_1 s_1) \right. \\ &\quad \left. - \int d\mathbf{r}_2 \frac{\psi_j^*(\mathbf{r}_2 s_2)}{|\mathbf{r}_1 - \mathbf{r}_2|} P_{12} \psi_j(\mathbf{r}_2 s_2) \psi_i(\mathbf{r}_1 s_1) \right] = \varepsilon_i \psi_i(\mathbf{r}_1 s_1). \end{aligned} \quad (7b)$$

Since the Fock operator depends on the set of orbitals $\{\psi_i\}$ which we would like to obtain as solutions, HF equations are nonlinear equations; in contrast to that the original Schrödinger equation for the N electron systems is a linear one. This difference affects the scheme to solve the equation and the symmetry of the solutions. First, since a set of orbitals $\{\psi_i\}$ is needed to construct the Fock operator, we must decide the initial orbitals $\{\psi_i\}$ and the HF equations must be solved in an iterative manner. Second, the HF effective Hamiltonian is not determined a priori, but is given by the users. In quantum mechanics, the Hamiltonian determines the symmetry of the problem, so that we set up the symmetry framework of the HF approximation when we give the set of initial orbitals. This feature of HF approximation often results in broken-symmetry solutions, which violate a condition of a correct solution of ab initio Hamiltonian given by Eq. 4. The HF approximation allowing the broken-symmetry solutions with collinear spin alignments,^{6,15–21} is called unrestricted HF (UHF), in contrast with the symmetry-restricted HF that is denoted as RHF. The generalized version of HF approximation, which employs the general spin orbitals (GSOs) to allow spin-canting,^{22–25} is called the generalized HF (GHF) approximation. We here note that Eqs. 6 and 7 are for GHF, in contrast to the standard formulation⁶ in which the spin variables are reduced. The GSO is a superposition of α and β states as

$$\psi_i(\mathbf{x}) = \begin{pmatrix} \psi_i(\mathbf{r}\alpha) \\ \psi_i(\mathbf{r}\beta) \end{pmatrix} = \begin{pmatrix} \psi_i^\alpha(\mathbf{r}) \\ \psi_i^\beta(\mathbf{r}) \end{pmatrix}. \quad (9)$$

The corresponding first-order reduced spin density matrix (1-DM) includes not only spinless part $\rho(\mathbf{r}; \mathbf{r}')$, but also, x, y, z -components of spin density matrices $\{\rho_m(\mathbf{r}; \mathbf{r}')\}_{m=x, y, z}$:

$$\rho_s(\mathbf{r}; \mathbf{r}') = \sum_i \begin{pmatrix} \psi_i^\alpha(\mathbf{r}) \psi_i^{\alpha*}(\mathbf{r}') & \psi_i^\alpha(\mathbf{r}) \psi_i^{\beta*}(\mathbf{r}') \\ \psi_i^\beta(\mathbf{r}) \psi_i^{\alpha*}(\mathbf{r}') & \psi_i^\beta(\mathbf{r}) \psi_i^{\beta*}(\mathbf{r}') \end{pmatrix}$$

$$= \begin{pmatrix} \rho_{\alpha\alpha}(\mathbf{r}; \mathbf{r}') & \rho_{\alpha\beta}(\mathbf{r}; \mathbf{r}') \\ \rho_{\beta\alpha}(\mathbf{r}; \mathbf{r}') & \rho_{\beta\beta}(\mathbf{r}; \mathbf{r}') \end{pmatrix} = \begin{pmatrix} \frac{\rho(\mathbf{r}; \mathbf{r}')}{2} + \rho_z(\mathbf{r}; \mathbf{r}') & \rho_x(\mathbf{r}; \mathbf{r}') - i\rho_y(\mathbf{r}; \mathbf{r}') \\ \rho_x(\mathbf{r}; \mathbf{r}') + i\rho_y(\mathbf{r}; \mathbf{r}') & \frac{\rho(\mathbf{r}; \mathbf{r}')}{2} - \rho_z(\mathbf{r}; \mathbf{r}') \end{pmatrix}. \quad (10)$$

We again note here that the 1-DMs of UHF solutions reduce to two diagonal terms of right side of Eq. 10. Thus, the employment of GSO is essential in order to describe the full spin degree of freedom of canting-spin systems. We described the theoretical background of GHF in the next section.

The Role of Broken-Symmetry of GHF Solutions on Description of Physical Phenomena

While many quantum chemists reasonably hesitated to use the UHF or GHF approaches due to their fundamental defects concerning symmetry, some pioneers opened up the field of “broken-symmetry quantum chemistry”.^{15–27} As for fundamental aspects, Fukutome²⁴ classified all possible types of GHF solutions from the viewpoint of spin-rotational (S) and time reversal (T) groups. As described in the preceding section, users can determine the symmetry framework of the HF solutions. If one chooses a $S \times T$ symmetry-allowed (SA) initial guess, the HF equation gives a SA solution. On the other hand, when we start from a trial MO having no symmetry of $S \times T$, a fully broken-symmetry solution might be obtained. However, if a trial MO has symmetry of a subgroup of $S \times T$, which we denoted here as G, a symmetry restriction of a GHF solution also follows the symmetry of the group G. All eight subgroups {G} of $S \times T$ are derived and those first-order reduced density matrices of the corresponding eight types of GHF solutions are analyzed from the standpoints of physical properties. All types of

GHF solutions are listed in Fig. 1; these are the same as those in paper²⁴ except that we use the term “helical spin density wave (HSDW)” instead of torsional spin density wave (TSDW). In Fig. 1, we also present the physical fundamental variables of each class in the real space representation, instead of in the density matrix form written in the original paper, in order to connect to the discussion of GSO-DFT provided in later sections. These fundamental variables imply the physical functionality of the corresponding state. The $\{\rho_m(\mathbf{r})\}_{m=x,y,z}$ are spin densities so that the corresponding state exhibits magnetism. If the R_X includes $\vec{J}_\rho(\mathbf{r})$ and $\{\vec{J}_{S_m}(\mathbf{r})\}_{m=x,y,z}$, the corresponding electronic structure involves charge current and spin currents, respectively. This classification of GHF solutions was extended to include the spatial point group (P), i.e., to $P \times S \times T$, by Ozaki and Fukutome.²⁵ Ozaki further developed the classification of Hartree–Fock–Bogoliubov (HFB) solutions²⁶ in order to analyze the superconductivity states. On the other hand, K. Yamaguchi et al.²⁷ added the permutation symmetry (P_n) to $P \times S \times T$, and discussed the interrelationships among the HF theory, the Heisenberg model, the Hückel theory, and the extended HF theory, from the viewpoint of $P_n \times P \times S \times T$ symmetry.

The classification of GHF covers most of electronic states while conserving the electron numbers. Properties can be described by using one-electron density matrix: charge density wave (CDW), charge current wave (CCW), spin current wave (SCW), one-dimensional (1D), two-dimensional (2D), and three-dimensional (3D) spin density waves (SDWs). In other words, these states can be described by using GHF approximations.

The Role of Broken-Symmetry of GHF Solutions on Electron Correlation

In this section, we discuss the electron correlation, which can be covered by the spin-restricted and spin unrestricted HF solu-

Time-reversal invariant closed shell (TICS)		Charge current wave (CCW)
$R_{\text{TICS}}(\mathbf{r}) = \{\rho(\mathbf{r})\}$		$R_{\text{CCW}}(\mathbf{r}) = \{\rho(\mathbf{r}), \vec{J}_\rho(\mathbf{r})\}$
Axial spin current wave (ASCW)	Axial spin density wave (ASDW)	Axial spin wave (ASW)
$R_{\text{ASCW}} = \{\rho(\mathbf{r}), J_{S_z}(\mathbf{r})\}$	$R_{\text{ASDW}} = \{\rho(\mathbf{r}), \rho_x(\mathbf{r})\}$	$R_{\text{ASW}} = \{\rho(\mathbf{r}), \rho_z(\mathbf{r}), \vec{J}_\rho(\mathbf{r}), \vec{J}_{S_z}(\mathbf{r})\}$
Torsional spin current wave (TSCW)	Helical spin density wave (HSDW)	Torsional spin wave (TSW)
$R_{\text{TSCW}} = \{\rho(\mathbf{r}), \rho_x(\mathbf{r}), \vec{J}_S(\mathbf{r})\}$	$R_{\text{HSDW}} = \{\rho(\mathbf{r}), \rho_x(\mathbf{r}), \rho_z(\mathbf{r}), J_{S_y}(\mathbf{r})\}$	$R_{\text{TSW}} = \{\rho(\mathbf{r}), \rho_x(\mathbf{r}), \rho_y(\mathbf{r}), \rho_z(\mathbf{r}), \vec{J}_\rho(\mathbf{r}), \vec{J}_S(\mathbf{r})\}$

Fig. 1. The classification of GSO solutions and the corresponding set of fundamental physical variables, R. Here $\rho(\mathbf{r})$, $\vec{J}_\rho(\mathbf{r})$, $\{\rho_m(\mathbf{r})\}_{m=x,y,z}$ are the electron density, the charge current, and the spin densities of a direction m , respectively. $J_{S_m}(\mathbf{r})$ and $\vec{J}_S(\mathbf{r})$ are spin currents with the fixed direction, m , and of three-dimensional, respectively.

tions. The electron–electron interaction term can be expressed as

$$V_{ee} = \sum_{s_1, s_2} \iint d\mathbf{r}_1 d\mathbf{r}_2 \frac{1}{|\mathbf{r}_1 - \mathbf{r}_2|} \rho_2(\mathbf{x}_1, \mathbf{x}_2), \quad (11)$$

by using the second-order reduced density matrix (2-DM) defined by,

$$\rho_2(\mathbf{x}_1, \mathbf{x}_2) = \frac{N(N-1)}{2} \iint d\mathbf{x}_3 \dots d\mathbf{x}_N |\Psi(\mathbf{x}_1, \mathbf{x}_2, \mathbf{x}_3, \dots, \mathbf{x}_N)|^2. \quad (12)$$

Under the GHF approximation, $\rho_2(\mathbf{x}_1, \mathbf{x}_2)$ can be expanded by first order reduced density matrix $\rho_1(\mathbf{x}_1; \mathbf{x}_2)$ and spin density matrix $\rho_1(\mathbf{x})$ as

$$\rho_2(\mathbf{x}_1, \mathbf{x}_2) = \frac{1}{2} (\rho_1(\mathbf{x}_1) \rho_1(\mathbf{x}_2) - \rho_1(\mathbf{x}_1; \mathbf{x}_2) \rho_1(\mathbf{x}_2; \mathbf{x}_1)). \quad (13)$$

By substituting the first term into Eq. 11, we obtain the classical coulomb interaction:

$$E_{clmb} = \frac{1}{2} \iint d\mathbf{r}_1 d\mathbf{r}_2 \frac{\rho(\mathbf{r}_1) \rho(\mathbf{r}_2)}{|\mathbf{r}_1 - \mathbf{r}_2|}. \quad (14a)$$

On the other hand, the last term leads to the exchange interaction,

$$E_x = - \iint d\mathbf{r}_1 d\mathbf{r}_2 \frac{1}{|\mathbf{r}_1 - \mathbf{r}_2|} \times \left\{ \frac{1}{4} \rho_1(\mathbf{r}_1; \mathbf{r}_2) \rho_1(\mathbf{r}_2; \mathbf{r}_1) + \sum_m^{x,y,z} \rho_m(\mathbf{r}_1; \mathbf{r}_2) \rho_m(\mathbf{r}_2; \mathbf{r}_1) \right\}. \quad (14b)$$

Here, $\rho_m(\mathbf{r}_1; \mathbf{r}_2)$ is a m -component spin density matrix. Thus $\rho_2(\mathbf{x}_1; \mathbf{x}_2)$, which is related to the electron interaction term given by Eq. 11, is rewritten as:

$$\sum_{s_1, s_2} \rho_2(\mathbf{x}_1, \mathbf{x}_2) = \frac{1}{2} \rho(\mathbf{r}_1) \rho(\mathbf{r}_2) - \frac{1}{4} \rho_1(\mathbf{r}_1; \mathbf{r}_2) \rho_1(\mathbf{r}_2; \mathbf{r}_1) - \sum_m^{x,y,z} \rho_m(\mathbf{r}_1; \mathbf{r}_2) \rho_m(\mathbf{r}_2; \mathbf{r}_1). \quad (15)$$

In the case of RHF solutions for closed shell systems, the third term on the right side of Eq. 15 vanishes and $\rho_2(\mathbf{x}_1, \mathbf{x}_2)$ reduces to spinless 2-DM, $\rho_2(\mathbf{r}_1, \mathbf{r}_2)$. Then we further divided $\rho_2(\mathbf{r}_1, \mathbf{r}_2)$ into that of parallel spin pairs, $\rho_2^{\sigma\sigma}(\mathbf{r}_1, \mathbf{r}_2) \equiv \rho_2(\mathbf{r}_1\sigma, \mathbf{r}_2\sigma)$ ($\sigma = \alpha$ or β), and that of antiparallel spin pairs, $\rho_2^{\alpha\beta}(\mathbf{r}_1, \mathbf{r}_2) \equiv \rho_2(\mathbf{r}_1\alpha, \mathbf{r}_2\beta)$ as:

$$\rho_2^{\sigma\sigma}(\mathbf{r}_1, \mathbf{r}_2) = \frac{1}{4} \rho(\mathbf{r}_1) \rho(\mathbf{r}_2) - \frac{1}{4} \rho_1(\mathbf{r}_1; \mathbf{r}_2) \rho_1(\mathbf{r}_2; \mathbf{r}_1), \quad (16a)$$

$$\rho_2^{\alpha\beta}(\mathbf{r}_1, \mathbf{r}_2) = \frac{1}{4} \rho(\mathbf{r}_1) \rho(\mathbf{r}_2). \quad (16b)$$

Now we should note that the on-top pair density (OTPD), $\rho_2(\mathbf{r}_1, \mathbf{r}_2)|_{\mathbf{r}_1=\mathbf{r}_2}$, which is the probability that two electrons co-exist should be equal to zero if the electron correlation is taken into account. Otherwise, the OTPD contributes to a positive energy of V_{ee} . Indeed, $\rho_2^{\sigma\sigma}(\mathbf{r}_1, \mathbf{r}_2)|_{\mathbf{r}_1=\mathbf{r}_2} = 0$, which implies that the electron correlation between parallel spin pairs are fully included in RHF solutions because we employed the Slater determinant given by Eq. 6. On the other hand, the OTPD for anti-

parallel spins becomes

$$\rho_2^{\alpha\beta}(\mathbf{r}, \mathbf{r}) = (\rho(\mathbf{r})/2)^2 = \rho^\alpha(\mathbf{r}) \rho^\beta(\mathbf{r}). \quad (17)$$

This result implies that there are no correlation effects between different spins in RHF solutions. The failure of the RHF approach is ascribed to this Eq. 17. For instance, let us consider the dissociation curve of a hydrogen molecule with a minimal basis. If the two hydrogen atoms bond tightly, two electrons occupied the same bonding orbital:

$$\psi_{\text{bond}}(\mathbf{r}) = \frac{1}{\sqrt{2}} (\phi_1 + \phi_2)(\mathbf{r}), \quad (18a)$$

which is energetically favored due to the nuclear attraction and kinetic energy terms. Here a factor due to the overlap of AOs is omitted. However, as the interatomic distance increases, the coulomb interaction term between two electrons dominates over other terms, and the situation where two electrons are more or less localized on different atoms is expected to be stable. However, since in the RHF approximation there is no freedom to avoid the pair-occupancy as seen in Eq. 17, the dissociation of hydrogen molecule can not be described. Indeed, as shown in Fig. 2, the RHF solutions are good approximations to exact CI solutions, but become unstable as the interatomic distance increases.

On the other hand, a degree of freedom to mix the bonding orbital, ψ_{bond} and antibonding orbital,

$$\psi_{\text{antibond}}(\mathbf{r}) = \frac{1}{\sqrt{2}} (\phi_1 - \phi_2)(\mathbf{r}), \quad (18b)$$

can be introduced into the UHF solutions,

$$\phi^\alpha(\mathbf{r}) = \cos \theta \psi_{\text{bond}}(\mathbf{r}) + \sin \theta \psi_{\text{antibond}}(\mathbf{r}), \quad (19a)$$

$$\phi^\beta(\mathbf{r}) = \cos \theta \psi_{\text{bond}}(\mathbf{r}) - \sin \theta \psi_{\text{antibond}}(\mathbf{r}). \quad (19b)$$

Here the range of θ is given by $0 \leq \theta \leq \frac{\pi}{4}$. Both UHF orbitals given by Eq. 19 reduce to that of Eq. 18a if $\theta = 0$, while $\theta = \pi/4$ corresponds to the completely dissociated hydrogen atoms. The contributions to 2-DM from parallel and antiparallel spin pairs become

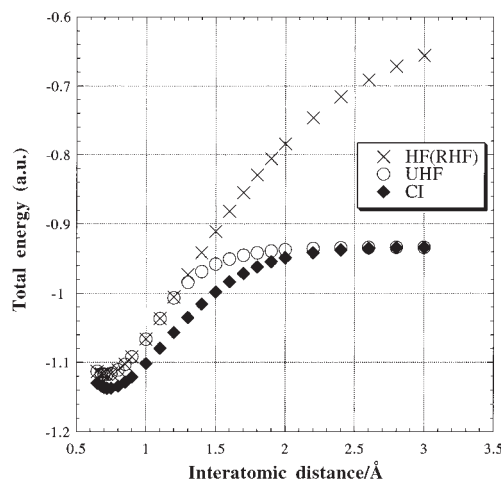


Fig. 2. Potential curves of a hydrogen molecule calculated by RHF, UHF, and CI methods with the minimal (STO-3G) basis set.

$$\rho_2^{\sigma\sigma}(\mathbf{r}_1, \mathbf{r}_2) = \rho^\sigma(\mathbf{r}_1)\rho^\sigma(\mathbf{r}_2) - \rho_1^\sigma(\mathbf{r}_1; \mathbf{r}_2)\rho_1^\sigma(\mathbf{r}_2; \mathbf{r}_1) \quad (20a)$$

$$\begin{aligned} \rho_2^{\alpha\beta}(\mathbf{r}_1, \mathbf{r}_2) &= \frac{1}{2}\rho^\alpha(\mathbf{r}_1)\rho^\beta(\mathbf{r}_2) \\ &= \frac{1}{2}\left(\frac{1}{4}\rho(\mathbf{r}_1)\rho(\mathbf{r}_2) - \rho^z(\mathbf{r}_1)\rho^z(\mathbf{r}_2)\right). \end{aligned} \quad (20b)$$

The most remarkable feature is that OTPD between antiparallel spins, $\rho_2^{\alpha\beta}(\mathbf{r}_1, \mathbf{r}_2)|_{\mathbf{r}_1=\mathbf{r}_2}$, decreases as the electrons are localized to two different atoms. At $\theta = \pi/4$, $\rho_2^{\alpha\beta}(\mathbf{r}_1, \mathbf{r}_2)|_{\mathbf{r}_1=\mathbf{r}_2}$ becomes zero, achieving the complete treatment of the electron correlation between α and β electrons. Indeed, UHF solutions show the correct dissociation behavior of hydrogen molecule and give the same results as CI ones at the dissociation limit as shown in Fig. 2.

Here we note that the spin density, $\rho^z(\mathbf{r})$, which appears in Eq. 20b plays an essential role in the electron correlation of the UHF approximation. Now we consider the singlet state of hydrogen molecule, so that this indicates that we utilize the broken-symmetry feature of the HF approximation to reproduce the good pair correlation. This relation between the symmetry density of the GHF approximation and the electron correlation was first discussed by Yamaguchi in 1978.²⁸ As described below, similar logic was applied for Kohn–Sham solutions by Perdew et al. in 1995 to escape the symmetry-dilemma of KS-DFT.²⁹

It should be commented that the electron correlation effects covered by the UHF approximation are limited to those between electrons that occupy the same orbitals in the RHF limit. If we employ the GHF approximation, the number of electrons that correlate with each other might be considerably extended. However, that situation is only for the case of spin-frustrated or spin-degenerated cases described below. So, usually, we must apply an expansion of a wavefunction described in order to take the electron correlation into account.

Symmetry-Adapted Approaches Based on an Expansion of a Wavefunction

The HF approximation never gives an exact solution except for the noninteracting case. Usually an exact solution is expressed as a linear combination between a RHF configuration and all symmetry-adapted excited configurations:⁶

$$\Psi = C^{\text{HF}}\Phi^{\text{HF}} + \sum_{ar} C_a^r \Phi_a^r + \sum_{abrs} C_{ab}^{rs} \Phi_{ab}^{rs} + \sum_{abcrst} C_{abc}^{rst} \Phi_{abc}^{rst} + \dots, \quad (21)$$

where the first term is the RHF configuration, Φ_a^r is a singly excited one, Φ_{ab}^{rs} is a doubly excited one, etc. The expansion coefficients are determined to satisfy Eq. 3, usually by diagonalizing the Hamiltonian matrix. This exact approach is denoted by full configuration interaction (CI). The full CI is also not feasible even for a small molecule such as a benzene molecule, because the number of terms at the right side of Eq. 20 becomes enormous in general. Thus the truncation of the expansion is usually done, leading to CI double (CID), or CI single-and-double (CISD), etc. The most widely used wavefunction is the complete-active-space (CAS) based wavefunction.³⁰ To construct a CAS wavefunction, we must divide MO's into three spaces by judging from the occupied and virtual orbital ener-

gies of HF solutions. Canonical orbitals near the HOMO and LUMO are chosen as CAS orbitals, while MOs having much lower energies than HOMO, and those much higher than LUMO are classified into core orbitals and virtual orbitals, respectively. Then, the CAS wavefunction is obtained by expanding all configurations within CAS orbitals:

$$\Psi^{\text{CAS}} = C^{\text{HF}}\Phi^{\text{HF}} + \sum_i^{\text{All excitations within CAS space}} C_i \Phi_i. \quad (22)$$

One key point of CAS-based approaches is the selection of the active space. As for the molecular magnetic systems, we apply the UHF natural orbitals (NOs)^{31–35} which are obtained by diagonalizing the electron density of UHF solutions as $\rho(\mathbf{r}) = \sum_i n_i |\phi_i(\mathbf{r})|^2$. Occupation numbers of UNOs for radical species, $\{n_i\}$, dictate three groups of UNOs for CAS computations. Almost doubly- and un-occupied UNOs are treated as core and virtual orbitals, respectively; neither of these contribute any magnetic properties in the corresponding UHF solution. The UNOs having a fractional occupation number ($0 < n_i < 2.0$) are mainly responsible for the non-dynamical correlations of target species, which are results of degenerate or near-degenerate effects, so that are appropriate for active orbitals of CASCI or CASSCF. The extension from UNO to GHF NO is trivial.

For the qualitative discussion of nondynamical effects and the state specific characters such as ionic and/or radical, CASCI or CASSCF approaches are effective if the CAS is appropriately large. This is because all of the resonance states to stabilize the electronic state can be included if the CAS covers the full valence orbitals. Indeed, we examined whether the spin-crossovers occurred for hole-doped bis-and-tris(methylene)-amines³⁴ and hole-doped polycarbenes³⁵ by carrying out CASSCF calculations; these were consistent with the qualitative discussion based on spin polarization-and-delocalization rules and with an experimental result. For instance, the four essential valence bond structures of the doublet spin state *meta*-phenylene bis(methylene) shown in Fig. 3, one of which corresponds to an UHF solution, can be included with CASSCF solutions.³⁵ Further, for quantitative purposes, we show that the second-order perturbation method (PT2) based on CASSCF (CASPT2)³⁶ gave the highly qualitative results for estimation of effective exchange interactions of simple radical systems such as the hydrogen cluster,³² the dimer of triplet methylenes,³³ and the organic ion-radical cited above.^{34,35}

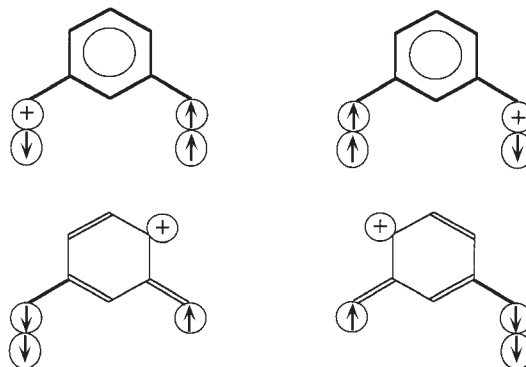


Fig. 3. The important VB structures for the doublet state of the *meta*-phenylene bis(methylene).

However, there is a problem concerning the computational costs in these CAS based methods. In order to expand the wavefunction fully for the systems involving many active electrons-and-spaces, huge computer resources are needed. To resolve this problem, the fragment MO approach³⁷ of the CAS based methods, which has been recently developed, seems to be a most promising direction of ab initio WFT towards macromolecules. However, if the active electrons-and-orbitals are localized in the small and functional unit, as in the case of single molecular magnets like Mn₁₂Ac,³⁸ of which the number of active electrons is more than 40, a CAS computation of this fragment will be not feasible. Thus, the use of the DFT is the only measure left for such cases.

Generalized Spin Orbital Density Functional Theory

In the Hohenberg–Kohn theorem and its extension of spin variables,^{39–43} the fundamental parameter of an N-electrons system is the spin density, which is the spatial diagonal part of $\rho_s(\mathbf{r}, \mathbf{r}')$ given in Eq. 10:

$$\begin{aligned}\rho_s(\mathbf{r}) &= \begin{pmatrix} \rho_{\alpha\alpha}(\mathbf{r}) & \rho_{\alpha\beta}(\mathbf{r}) \\ \rho_{\beta\alpha}(\mathbf{r}) & \rho_{\beta\beta}(\mathbf{r}) \end{pmatrix} \\ &= \frac{\rho(\mathbf{r})}{2} \mathbf{E} + \sum_m^{x,y,z} \rho_m(\mathbf{r}) \sigma_m.\end{aligned}\quad (23)$$

Here \mathbf{E} is a unit matrix and $\{\sigma_m\}_{m=x,y,z}$ are Pauli matrices. We note that the dimension of the fundamental variable reduces to 3 from 3N of WFT. According to Levy's formulation, the ground state energy is determined by minimizing over the space of all N-representable spin densities:^{42,43}

$$E = \min_{\rho_s(\mathbf{r}) \rightarrow N} \left\{ F[\rho_s(\mathbf{r})] + \int d\mathbf{r} Tr V_{ext}(\mathbf{r}) \rho_s(\mathbf{r}) \right\}, \quad (24)$$

where $V_{ext}(\mathbf{r})$ is the coordinate representation of the external potential operator \hat{V}_{ext} . $F[\rho(\mathbf{r})]$ is the universal functional which is defined as

$$F[\rho_s(\mathbf{r})] = \min_{\Psi \rightarrow \rho_s(\mathbf{r})} \langle \Psi | \hat{T} + \hat{V}_{ee} | \Psi \rangle, \quad (25)$$

where \hat{T} and \hat{V}_{ee} are the kinetic energy and electron repulsion operators, respectively. The Euler equation becomes

$$\frac{\delta F[\rho_s(\mathbf{r})]}{\delta \rho_{\sigma_2\sigma_1}(\mathbf{r})} = -V_{ext}^{\sigma_1\sigma_2}(\mathbf{r}) + \delta_{\sigma_1\sigma_2} \mu. \quad (26)$$

This is the original equation in DFT, but we do not know the form of $F[\rho_s(\mathbf{r})]$ to be solved. The symmetry of the spin density, as well as that of the wavefunction, is restricted by a given $V_{ext}(\mathbf{r})$.

On the other hand, the KS system is based on the minimizing of the kinetic energy functional,

$$\begin{aligned}T_s[\rho_s(\mathbf{r})] &= \min_{\Phi \rightarrow \rho_s(\mathbf{r})} \langle \Phi | \hat{T} | \Phi \rangle \\ &= \sum_{i=1}^N \langle \psi_i | -\frac{\nabla_i^2}{2} | \psi_i \rangle.\end{aligned}\quad (27)$$

Thus, the auxiliary KS wavefunction become the SD one, introducing a noninteracting picture of the KS theory. Through the Euler equation which is derived from Eq. 27,

$$\frac{\delta T_s[\rho_s(\mathbf{r})]}{\delta \rho_{\sigma_1\sigma_2}(\mathbf{r})} = -V_{eff}^{\sigma_1\sigma_2}(\mathbf{r}) + \delta_{\sigma_1\sigma_2} \mu. \quad (28)$$

The minimization of the expectation value of the KS Hamiltonian is given by

$$\begin{aligned}E_s &= \min_{\rho_s(\mathbf{r}) \rightarrow N} \left\{ T_s[\rho_s(\mathbf{r})] + \int d\mathbf{r} Tr V_{eff}(\mathbf{r}) \rho_s(\mathbf{r}) \right\} \\ &= \min_{\Phi(\mathbf{r}) \rightarrow N} \langle \Phi | \hat{T}_s + \hat{V}_{eff} | \Phi \rangle.\end{aligned}\quad (29)$$

By substituting the relation,

$$T_s[\rho_s(\mathbf{r})] = F[\rho_s(\mathbf{r})] - J[\rho_s(\mathbf{r})] - E_{xc}[\rho_s(\mathbf{r})], \quad (30)$$

where $J[\rho_s(\mathbf{r})]$ is the classical coulomb term and $E_{xc}[\rho_s(\mathbf{r})]$ is the XC functional, into the Eq. 28 and using Eq. 26, one obtains this KS effective potential:

$$V_{eff}^{\sigma_1\sigma_2}(\mathbf{r}) = V_{ext}^{\sigma_1\sigma_2}(\mathbf{r}) + \delta_{\sigma_1\sigma_2} \int d\mathbf{r}' \frac{n(\mathbf{r}')}{|\mathbf{r} - \mathbf{r}'|} + \frac{\delta E_{xc}[\rho_s(\mathbf{r})]}{\delta \rho_{\sigma_2\sigma_1}(\mathbf{r})}. \quad (31)$$

Thus the set of equations for KS orbitals that appeared in the second line of Eq. 27 becomes

$$\begin{aligned}\sum_{\sigma_2} \left[\delta_{\sigma_1\sigma_2} \left\{ -\frac{\nabla_i^2}{2} + \int d\mathbf{r}' \frac{n(\mathbf{r}')}{|\mathbf{r} - \mathbf{r}'|} \right\} \right. \\ \left. + \frac{\delta E_{xc}}{\delta \rho_{\sigma_2\sigma_1}}(\mathbf{r}) + V_{ext}^{\sigma_1\sigma_2}(\mathbf{r}) \right] \psi_i^{\sigma_2}(\mathbf{r}) = \varepsilon_i \psi_i^{\sigma_1}(\mathbf{r}).\end{aligned}\quad (32)$$

If an external magnetic field is absent, $V_{ext}(\mathbf{r})$ reduces to the nuclear attraction potential so that the GSO treatment described in this section might be meaningless. Is this statement true? The problem is whether the exact spin-allowed solution can be always obtained in principle. We discuss the validity of the KS theory in relation to this problem in the next section.

Instability, Symmetry-Breaking and General Density Functional Theory for Strongly Correlated Electron Systems

Many KS-DFT users know from their experience that the spin polarization often occurs for a homolysis of a chemical bond, or for an antiferromagnetic state of a solid, even in the case of the singlet state without no external field. Obviously, this is incorrect from the viewpoint of nonrelativistic quantum mechanics. This broken-symmetry feature of KS theory is a more serious problem than that of the HF approximation because, in contrast to the HF approximation, the KS-DFT is thought to be “exact” theory “without approximation”, at least in principle. Towards a more accurate KS-DFT, the essential part of the KS theory, i.e., exchange-correlation (XC) functional has been improved step by step: starting from the local spin density approximation (LSDA),⁴⁴ the generalized gradient approximation (GGA)^{45,46} involving gradient correction terms, the meta-GGA,⁴⁷ and now the hybrid methods⁴⁸ which are combining LSDA, GGA with the HF approximation, are most widely used. Here some fundamental questions arise: why do the broken-symmetry solutions often become stable for strong correlated systems, although the KS theory is an exact theory in principle? If the cause of all defaults is the “approximated”

XC functional, will a series of such improvements on the XC functional lead to the “exact” XC functional of the KS theory in the future, by which we can obtain the spin-symmetry adapted KS solutions for magnetic systems? From the standpoint of quantum chemists, these questions are inevitable in applications of KS-DFT for strongly correlated systems.

Here, we consider the H_2 molecule within the minimal basis set as an example. In this case, the density is expressed by natural orbitals (NOs) as

$$\rho(\mathbf{r}) = n\psi_{\text{bond}}(\mathbf{r})^2 + (2 - n)\psi_{\text{antibond}}(\mathbf{r})^2. \quad (33)$$

Here ψ_{bond} and ψ_{antibond} are bond and anti-bond NOs, respectively. Here we employed the minimal basis and there is no freedom for the orbital relaxation, so that the functional shapes of bonding and antibonding orbitals are uniquely given by Eq. 18. In addition, the sum of occupation numbers is 2. Thus there is a one-to-one correspondence between occupation number of a bond NO, n , and density, $\rho(\mathbf{r})$. So, if the KS theory is exact, the occupation number of the calculated NOs must be equal to those of CI. In the KS picture for any closed-shell molecule, an occupation number of a KS orbital is always equal to 2 (occupied) or to 0 (unoccupied), for it is an occupation number of its natural orbital, as shown in Fig. 4. On the other hand, the occupation numbers of bonding NOs of CI solutions become fractional due to many-body effects over the whole region of interatomic distances. As described above, the couple of natural orbitals of KS solutions are equal to those of CI solutions:

$$\psi_{\text{bond}}(\mathbf{r}) = \psi_{\text{bond}}^{\text{KS}}(\mathbf{r}) = \psi_{\text{bond}}^{\text{CI}}(\mathbf{r}), \quad (34a)$$

$$\psi_{\text{antibond}}(\mathbf{r}) = \psi_{\text{antibond}}^{\text{KS}}(\mathbf{r}) = \psi_{\text{antibond}}^{\text{CI}}(\mathbf{r}). \quad (34b)$$

Thus, the difference in the occupation number between KS solutions and CI solutions implies that KS theory provides the incorrect density for this case, unless $|\psi_{\text{bond}}(\mathbf{r})| = |\psi_{\text{antibond}}(\mathbf{r})|$ that would yield a nonbonding density.

Here we note that this situation can never be improved by any change on the XC functional. In other words, there is no “exact XC functional” of the KS theory, by which the exact

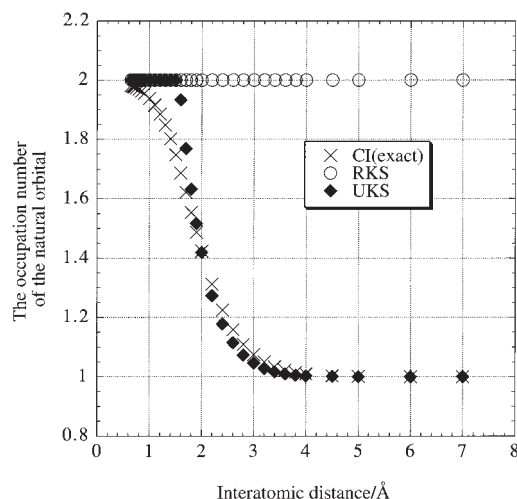


Fig. 4. The occupation numbers of RKS, UKS, and CI solutions for dissociation curves of a hydrogen molecule with the STO-3G basis set.

density is obtained. The reason for this failure of KS theory is ascribed not to the approximated XC functional, but to the noninteracting picture that is the theoretical framework of KS theory. The density given by Eq. 33 with fractional occupation numbers (FONs) is beyond the scope of KS theory. In order to assess the validity of the electronic structure theory, we should also take the influence of the basis set into account; we do not intend to prove the invalidity of the KS theory in general by taking this example. However, as is widely known, the hydrogen molecule with the minimal basis is a most fundamental system exhibiting a chemical bond. Thus, the failure of KS theory for this system implies that the KS theory is not always an “exact” or “accurate” theory in the actual quantum chemistry calculations.

Further, we should emphasize that KS solutions approximated well to the exact solutions near the equilibrium distance, while the differences between KS and CI solutions become remarkable as the interatomic distance increases, as shown in Fig. 4. The dissociated hydrogen molecule is the simplest model for the diradical systems, so that we anticipate that the KS theory will not work well for such cases even as an approximated theory. Indeed, many researchers pointed out the failure of the KS theory for diradical systems and intended to develop new electronic structure theories such as FON-DFT^{49–51} and CAS-DFT,^{52–54} in which the CAS-WFT and KS-DFT are combined.

On the other hand, in most of the KS-DFT calculations for magnetic systems, we usually remove the restriction of the double occupation in one orbital and employ the different-orbital-for-different-spin (DODS) picture in a similar manner to the UHF approximation. In fact, as shown in Fig. 4, the unrestricted KS (UKS) results gave excellent agreement with the exact results on the occupation numbers and also those on densities, by employing the “DODS type” MO. Here we employed the GGA-II functional⁴⁶ as a XC functional, but similar improvements are also observed for all of standard XC functionals. These remarkably good densities of UKS solutions arise from the non-zero θ in UKS orbitals as in the case of UHF orbitals:

$$\varphi^\alpha = \cos \theta \psi_{\text{bond}} + \sin \theta \psi_{\text{antibond}}, \quad (35a)$$

$$\varphi^\beta = \cos \theta \psi_{\text{bond}} - \sin \theta \psi_{\text{antibond}}. \quad (35b)$$

The corresponding density is given by

$$\rho(\mathbf{r}) = 2 \cos^2 \theta \psi_{\text{bond}}^2(\mathbf{r}) + 2 \sin^2 \theta \psi_{\text{antibond}}^2(\mathbf{r}), \quad (36)$$

presenting the FON character. However, it is also noted that the non-zero θ also yields the spin density:

$$\rho_z(\mathbf{r}) = 2 \sin 2\theta \psi_{\text{bond}}(\mathbf{r}) \psi_{\text{antibond}}(\mathbf{r}), \quad (37)$$

i.e., the broken-symmetry feature of UKS solutions is inevitable to reproduce the exact density. However, we would like to emphasize a positive aspect of Eq. 36: the parameter, θ , can be used to reproduce an exact density by exploiting the broken-symmetry feature of UKS solutions.

There remains another question: why is the spin-symmetry broken solution admissible in the KS theory? This problem arises from the mathematical features of the KS equation. That is, the KS equation becomes a non-linear equation, in contrast to that the original Schrödinger equation for many-electrons is a

linear equation, because the effective KS Hamiltonian depends on the KS solutions via a spin-density matrix in a manner similar to the case of HF approximation. In other words, the KS theory is also one of mean field theories so that the symmetry framework is determined not a priori, but by the initial spin density which is given by us. This fact is also proved mathematically by Görling.⁴⁰

Many theoretical researchers in the field of DFT struggled to resolve this spin-broken-symmetry problem. Görling proposed the symmetrized DFT by employing totally symmetrical part of spin density as the fundamental parameter.⁴⁰ On the other hand, Perdew et al. have suggested employing the on-top pair density (OTPD), $\rho_2(\mathbf{r}_1, \mathbf{r}_2)|_{\mathbf{r}_1=\mathbf{r}_2}$, as a fundamental parameter instead of the spin density in LSDA and GGA.²⁹ Their suggestion to utilize the OTPD is useful for interpretation of the spin-polarized solutions, because the OTPD is an important measure of solutions for electron correlations as shown by Yamaguchi.²⁸

We examined the validity of the KS theory for description of a simple chemical bond. Previously, fundamental defects of KS theory are reported for several other situations.^{55–57} One example is the multiplets of atoms, which were firstly suggested by von Barth.⁵⁵ He pointed out that the relative energies of multiplets of atoms could not be described by using the usual XC functional of KS method unless state-specific functionals are used. A FON scheme proposed by Filatov and Shaik⁵⁰ is such a system-dependent approach. Levy and Perdew proved that the convex sum of degenerate ground-state densities is not non-interacting v -representable,⁵⁶ providing a counterexample for the exactness of the KS theory. Many systems involving the degeneracy of the ground state configuration might be beyond the scope of the non-interacting picture of the KS theory. Savin⁵⁷ showed that the degeneracy problem in various chemical bonds required the ensemble density functional or the multi-determinantal wavefunction. He also argued the viability, as well as the limits, of the UKS approach based on the scenario of Ref. 29. We will present how the scope of the broken-symmetry DFT can be extended by use of GSO in a later section.

It seems reasonable to conclude from the discussion in this section that the UKS theory is not the exact DFT, but is an effective theory as a density-and-OTPD functional theory. A similar statement holds for GSO-DFT, since for a GSO solution the OTPD is improved as²⁸

$$\rho_2(\mathbf{r}, \mathbf{r}) = \frac{1}{4} \rho(\mathbf{r})^2 - \sum_m^{x,y,z} \rho_m(\mathbf{r})^2. \quad (38)$$

The spin broken-symmetry feature is useful to take the electron correlation into account for description of the density, OTPD, and energy, enabling us to describe the electronic structure of molecular magnetism.⁵¹ In addition, we have previously showed that the properties arising from the broken-symmetry, such as effective exchange effective integrals and spin densities, are useful pieces of information for comparison with the experimental results.⁵⁸

Consideration about the Symmetry of GSO-DFT

As described above, the initial spin densities constitute a symmetry framework of the KS equation. This situation is the same as the mean field approximation (MFA), for example, of the Heisenberg model,¹

$$\hat{H}_{HB} = - \sum_{i \neq j} J_{ij} \hat{S}_i \cdot \hat{S}_j \rightarrow \hat{H}_{HB}^{MFA} = - \sum_j \sum_{i(\neq j)} J_{ij} \langle \hat{S}_i \rangle \cdot \hat{S}_j. \quad (39)$$

The Hamiltonian on the right hand side implies that the symmetry of the effective Hamiltonian is determined by the initial spin densities $\{\langle \hat{S}_i \rangle\}$ and the given parameters of the effective exchange integrals $\{J_{ij}\}$. The symmetry framework of \hat{H}_{HB} is the product group of the spin-rotational (S) and time-reversal (T) groups. In contrast, the MFA leads to the classical spin picture because the Hamiltonian is the effective one to describe one-particle in the mean-field formed by other particles. Thus, the MFA solutions can be discussed using a magnetic symmetry.⁵⁹

It follows from this discussion that the classification of KS-DFT can also be achieved by utilizing the Fukutome symmetry. The GHF-type solutions of the KS equation have been discussed by Yamaguchi.⁶⁰ The classification of GHF of KS-auxiliary density matrices was discussed by Weiner and Trickey.⁶¹ We note here that the fundamental variables in KS-DFT are only spin densities and densities given by Eq. 23, which connected the symmetry and the search region of the spin DFT.⁶² The concrete types of KS solutions in the context of spin DFT can be listed as follows. The symmetric KS solution is called T-invariant closed shell (TICS)-type; it is a SA solution for $S \times T$. The collinear magnetic solution is invariant to a subgroup $A(\mathbf{e})M(\mathbf{e}')$, which we called axial spin density wave (ASDW). Here $A(\mathbf{e})$ is the subgroup of S consisting of all spin rotations around a fixed axis \mathbf{e} and $M(\mathbf{e}')$ is the group of order two generated by the T operation with the π spin rotation around a axis, \mathbf{e}' which is perpendicular to \mathbf{e} . HSDW and torsional spin wave (TSW) are noncollinear magnetic solutions which are invariant to $M(\mathbf{e})$ and identity element $\mathbf{1}$, respectively. Since the spin axis can be arbitrarily chosen for a spin-isotropic Hamiltonian, the relation

$$S \times T \supset A(\mathbf{e})M(\mathbf{e}') \supset M(\mathbf{e}') \supset \mathbf{1}, \quad (40)$$

holds. Since the elements of these subgroups give the restriction about the symmetry of the spin density, the relation for the search regions in the first line of Eq. 29 is

$$D_{TICS} \subset D_{ASDW} \subset D_{HSDW} \subset D_{TSW}, \quad (41)$$

D_{TICS} , D_{ASDW} , D_{HSDW} , and D_{TSW} are sets constituted of zero-, one-, two-, and three-dimensional spin densities respectively, as follows:

$$D_{TICS} \equiv \left\{ \rho_s(\mathbf{r}) = \frac{1}{2} \rho(\mathbf{r}) \mathbf{E}; \int d\mathbf{r} \text{Tr} \rho_s(\mathbf{r}) = N \right\}, \quad (42a)$$

$$D_{ASDW} \equiv \left\{ \rho_s(\mathbf{r}) = \frac{1}{2} \rho(\mathbf{r}) \mathbf{E} + \rho_z(\mathbf{r}) \sigma_z; \int d\mathbf{r} \text{Tr} \rho_s(\mathbf{r}) = N \right\}, \quad (42b)$$

$$D_{HSDW} \equiv \left\{ \rho_s(\mathbf{r}) = \frac{1}{2} \rho(\mathbf{r}) \mathbf{E} + \sum_m^{x,y,z} \rho_m(\mathbf{r}) \sigma_m; \int d\mathbf{r} \text{Tr} \rho_s(\mathbf{r}) = N \right\}, \quad (42c)$$

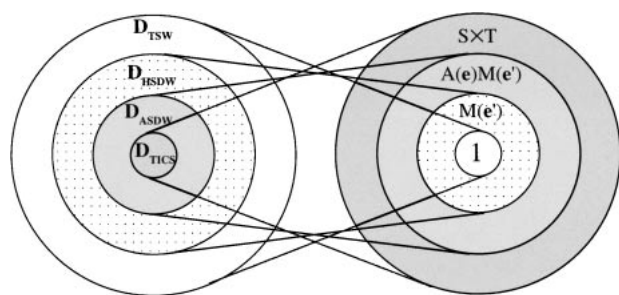


Fig. 5. The correspondence between the symmetry framework and the search region for GSO-DFT solutions. The right Venn diagram is of the symmetry groups the left one of search regions of GSO-DFT. As a symmetry restriction becomes more tight, the shade becomes deeper.

$$D_{TSW} \equiv \left\{ \rho_s(\mathbf{r}) = \frac{1}{2} \rho(\mathbf{r}) \mathbf{E} + \sum_m^{x,y,z} \rho_m(\mathbf{r}) \sigma_m; \int d\mathbf{r} \text{Tr} \rho_s(\mathbf{r}) = N \right\}. \quad (42d)$$

The correspondence between the symmetry framework and the search region of GSO-DFT is depicted in Fig. 5. We here neglect, for simplicity of the expression of D_{TICS} , a SA open-shell case in which a TICS solution always emerges as a more stable ASDW solution. We also omitted the auxiliary charge-current and spin-current⁶¹ in the HSDW and TSW solutions. The other subgroups enumerated in Fig. 1, which we do not describe in this section, will be essential for current and spin-DFT (CSDFT),⁶³ since the corresponding solutions exhibit the charge- and/or spin-currents. In particular, the charge currents are a fundamental variable when we describe the electron-transfer phenomena. The inclusion relation for the constrained search regions means that the higher symmetric solution can be obtained from a lower symmetric initial guess of KS equations. As is well known, even if we use a spin-unrestricted initial guess for a hydrogen molecule at the equilibrium geometry, we can automatically obtain the spin-restricted solution after the SCF convergence, since the TICS solution is also included in D_{ASDW} . However, since the spin density for the spin-unrestricted solution is not included in D_{TICS} , no ASDW solution can ever be obtained by choosing the TICS initial guess. There is a similar relation between collinear (D_{ASDW}) and noncollinear (D_{HSDW} or D_{TSW}) magnetic systems. Thus, employing a wider region with XC functional is essential for GSO-DFT.

In order to exploit D_{TSW} or D_{HSDW} as a search region, the XC function of the GSO-LSDA,^{39,64–68}

$$E_{XC}[\rho_+, \rho_-] = \int d\mathbf{r} (\rho_+(\mathbf{r}) + \rho_-(\mathbf{r})) \mathcal{E}(\rho_+(\mathbf{r}), \rho_-(\mathbf{r})) \quad (43)$$

must be employed for Eq. 32. Here it should be noted that the localized up- (ρ_+) and down- (ρ_-) spin densities are expressed not by ρ_α and ρ_β , but by

$$\rho_\pm(\mathbf{r}) = \rho(\mathbf{r}) \pm |\text{Tr} \vec{\sigma} \rho_s(\mathbf{r})|/2. \quad (44)$$

Here we should note that $\text{Tr} \vec{\sigma} \rho_s(\mathbf{r})/2 = (\rho_x, \rho_y, \rho_z)$ is a local spin. The extensions to GSO-GGA,^{69,70} GSO-SIC-DFT,⁷⁰ GSO-GW,⁷¹ and GSO-hybrid⁷² are straightforward. The unrestricted of the local spin directions means the extension of

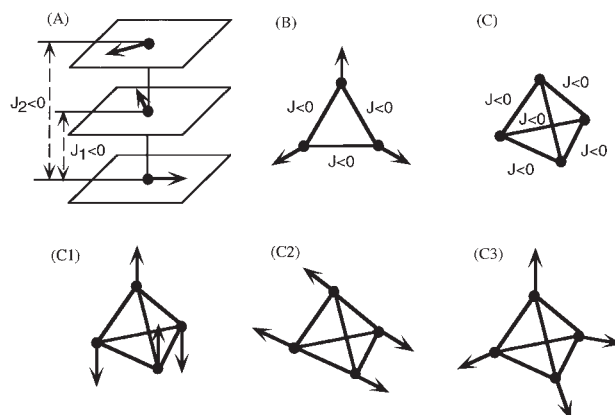


Fig. 6. Geometries and spin structures of the model systems. (A) The model of noncollinear magnetic system of 1D linear chain. (B) An equilateral triangular system and its stable spin structure. (C) The model system for tetrahedral spin clusters such as Fe_4S_4 and Mn_4O_4 . (C1) The ASDW state, (C2) the HSDW state, and (C3) the TSW state for the T_d cluster.

the search region from D_{ASDW} employed in the conventional LSDA scheme to D_{TSW} or D_{HSDW} in the GSO-LSDA scheme.

Several applications of GSO-DFT for noncollinear molecular magnetism are presented in the next section.

GSO-DFT Studies of Multicenter Clusters

The investigation of noncollinear magnetism has been started from the explanation in 1959 of the spiral spin state of MnO_2 by Yoshimori,⁷³ who used the classical Heisenberg (CHB) model.¹ For instance, the linear infinite chain of radical sources of which the nearest [J_1] and the next-nearest neighbor [J_2] effective exchange interactions compete with each other, is well known to be a helical spin density wave state (HSDW) as shown in Fig. 6(A). The first generation of the researchers concerning noncollinear magnetism analyzed the magnetism of solids in a similar manner.¹ The GSO-LSDA, which was first proposed by von Barth and Hedin³⁹ in 1972, has also been applied for HSDW states of solids.^{65,69} As for the molecular systems, in 1998, Oda et al. performed the GSO-LSDA computation for iron clusters by employing a planewave basis and an ultrasoft pseudopotential.⁶⁶ We also have performed the linear combination of gaussian-type orbital (LCGTO) computations of GSO-DFT for noncollinear molecular magnetic systems.^{62,67,68,70–72,74–76} In these studies we examined, by using ab initio GSO-DFT methods, several unfamiliar molecular magnetic states, some of which have been predicted by precursors.^{77–80} The first type of a noncollinear molecular magnetic system is a multicenter cluster exhibiting the spin-frustration. The simplest example is an equilateral triangular H_3 . GSO treatment of DFT is essential for this type of spin-frustrated systems in which competing exchange interactions lead to an energetically preferred 2D spin structure, as shown in Fig. 6(B). The stability of this type of HSDW state can be predicted by the CHB model, and indeed is confirmed for H_3 by GHF²² and GSO-DFT,⁷⁰ and for Cr_3 by GSO-DFT.⁷⁴ On the other hand, Yamaguchi et al.^{77,80} and Fukutome et al.⁷⁸ discussed a possible type of solution for tetrahedral clusters that is illustrat-

ed in Fig. 6(C). The CHB model of tetrahedral (T_d) type of clusters illustrated in Fig. 6(C) 3D spin structure provides the same energy for ASDW (Fig. 6(C1)), HSDW (Fig. 6(C2)), and TSW (Fig. 6(C3)) states. This system is thought to be the simplest model of the cubane clusters such as iron-sulfur clusters (Fe_4S_4) and manganese-oxide clusters (Mn_4O_4).⁸⁰ From the analysis of the magnetic susceptibility, it was reported that all values of effective integrals are negative for $[\text{Fe}_4\text{S}_4(\text{SPh})_4]^{n-}$ ($n = 2, 3$)⁸¹ and $(\text{C}_{12}\text{H}_{14}\text{N}_3\text{OMn(II)})_4\cdot 2\text{H}_2\text{O}$.⁸² The ASDW state of Fig. 6(C1) seems to be inappropriate, since it exhibits two local ferromagnetic couplings. Further, the precursors of GSO theories predicted the TSW state of Fig. 6(C3).^{78,79} However, it was reported that the HSDW of $\text{H}_4(T_d)$,⁷⁸ and the ASDW states of $\text{Fe}_4(T_d)$ ⁶⁶ become stable by GHF/INDO and GSO-LSDA, respectively. Thus, we first examined whether the TSW state becomes a most stable spin state. From our computation of LCGTO GSO-LSDA, we founded that the TSW state becomes more stable than the other two (ASDW and HSDW) states,⁶⁷ which is contrast with the previous calculational results presented by others,^{66,78} but is consistent with the fore-sights of some previous researchers.⁷⁷⁻⁷⁹ Further, for long interatomic distances of $\text{H}_4(T_d)$, all three states are nearly degenerate, so we speculated that the stability of the TSW state could be ascribed to the itinerant electron term rather than to exchange terms. In fact, the XC term of GSO-LSDA given by Eq. 43 does not depend on the local direction of spins, so that all spin states are degenerate if the orbital relaxation is neglected. Further, we discussed the role of the TSW spin structure in the reaction path for conserving the D_{2d} symmetry. The flexible spin structure of the TSW state is essential to interconnect continuously between the ASDW state of $\text{H}_4(D_{4h})$ and the HSDW state of perpendicular two hydrogen molecules, as shown in Fig. 7.

We also found that the TSW states are ground spin states for the cubane cluster, $\text{Mn}_4(\text{II})\text{O}_4$ ⁷² by using the GSO-LSDA, GSO-GGA, and GSO-Hybrid methods. These results are consistent with the experimental results of effective exchange integrals,⁸² while all spin states are nearly degenerate for $\text{Mn}_4(\text{II})$ without bridged anions, i.e., without the itinerant electrons. Furthermore, we found that TSW types of noncollinear molec-

ular magnetism become ground states for $\text{Cr}_4(T_d)$,⁷² bipyramidal Cr_5 ,⁷⁶ etc., at the ab initio GSO-DFT level.

In the real systems, there are some factors to disturb the stability of the 3D spin structures cited above. The small changes on the molecular structure owing to the Jahn–Teller (JT) effect or the asymmetric environment (ligands and proteins surrounding the cluster) are expected to make the low-dimensional spin ordering stable since these factors remove the spin degeneracy of the 1D- and/or 2D spin structures. Indeed, the molecular geometries described above have high-symmetries, which usually induce the JT distortion. Dzyaloshinsky–Moriya interactions due to spin–orbit effects and double-exchange interactions due to the mixed valency also provide other factors to change the spin-structure. Nevertheless, we conclude from our computational results that we need to incorporate at least three spin density variables to express the spin structure completely.

GSO-DFT Studies of Spin-Canting or Spin-Inversion Reactions

In recent ab initio studies of the magnetic materials, researchers often make use of the orbital degree of freedom.⁸³ For molecular magnetism, a spin alignment rule including non-biparticle organic systems and spin-intermediate states has been proposed by Yamaguchi.² Assigning a full spin degree of freedom to an orbital rather than to an atom or a molecule is expected to enable us to design the molecular magnetic systems in fine detail.

From the viewpoint of the chemical reaction, the orbital-and-spin coupled magnetism is related to spin-intermediate states and/or spin-inversion processes due to relativistic interaction. Although spin-canting and/or spin-inversion reactions are ubiquitous among oxidation reactions,⁸⁴ there was no appropriate ab initio treatment for those phenomena before our GSO-DFT study.⁶² Thus, we would like to present here the applicability of the GSO-DFT for cleavage of the oxygen molecule as a very simple example of those situations.

To clarify the story, we illustrate the spin structural changes of the oxygen-bond cleavage schematically in Fig. 8. As is well known, the chemical-bond of the triplet oxygen is different from others in that there are two ferromagnetically coupled

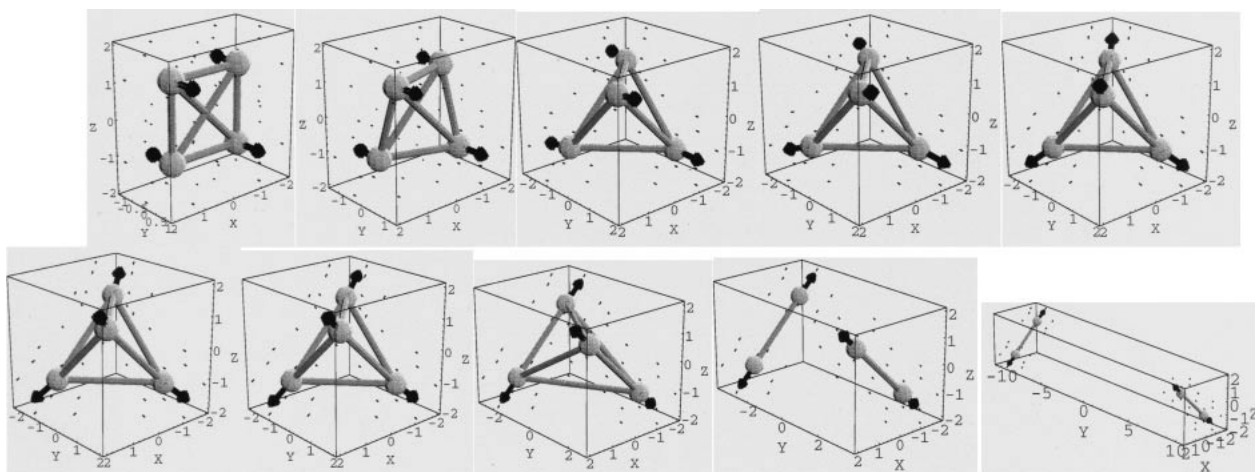


Fig. 7. Spin structural changes of H_4 as the reaction path conserving the D_{2d} symmetry.

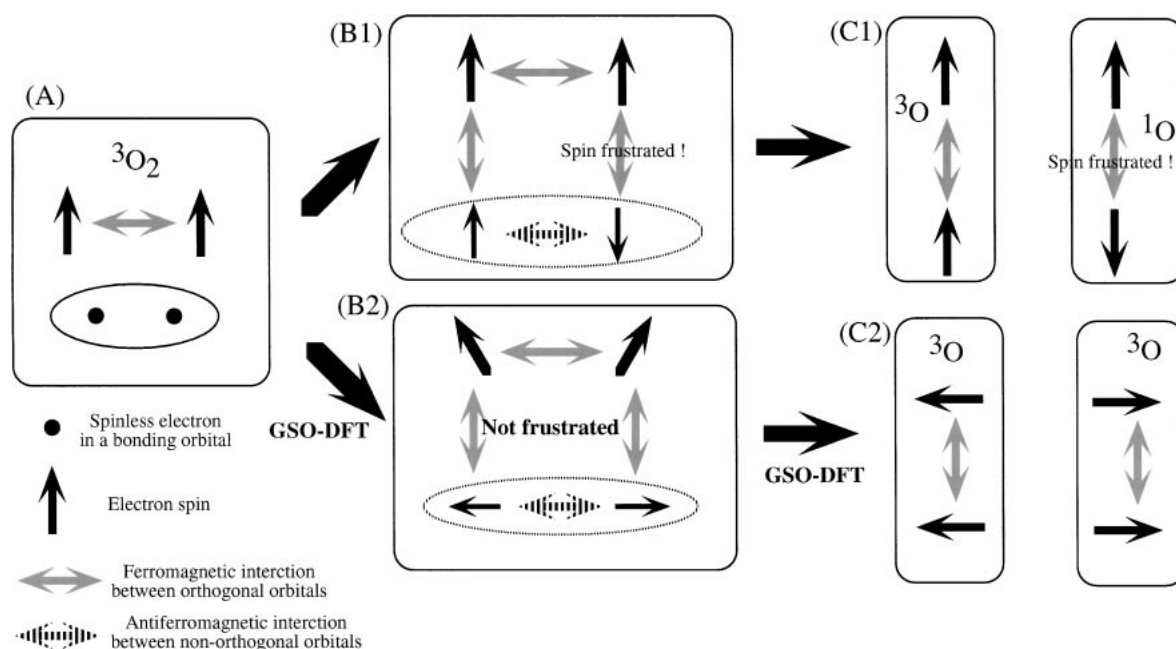


Fig. 8. Schematic scenario of spin-structural changes of the cleavage of oxygen molecule. (A) Spin structure of oxygen molecule. (B1) The intermediate and (C1) the dissociated states of oxygen molecule by using usual UKS-DFT. (B2) The intermediate and (C2) the dissociated two triplet oxygen atoms by using GSO-DFT.

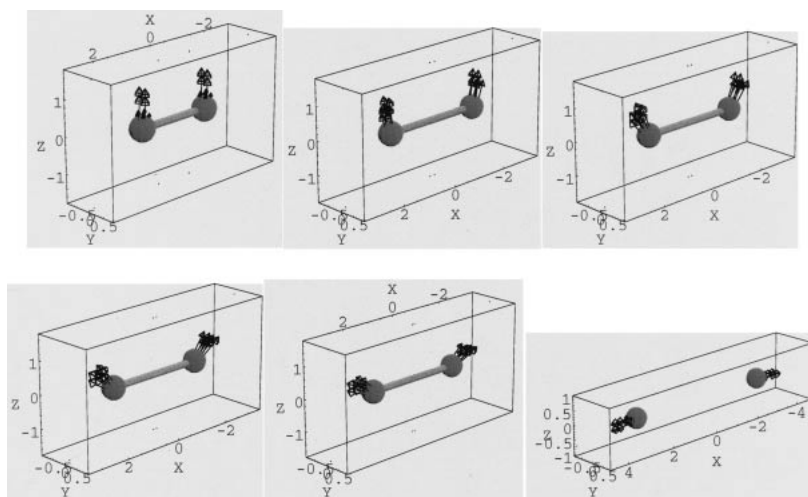


Fig. 9. The spin density plots of the oxygen cleavage calculated by GSO-B3LYP/6-31G**.

electrons (Fig. 8(A)) occupying the antibonding orbitals. As the σ bond dissociates, the usual DFT solutions suffer intra-atomic spin frustration, as shown in Fig. 8(B1), connecting to the excited dissociation limit consisting of a triplet oxygen atom and a singlet oxygen atom (Fig. 8(C1)). Thus, the general spin structure is expected to be necessary for the cleavage to avoid the spin-frustration, as shown in Fig. 8(B2), by which appropriately cleavage to two oxygen atoms in Fig. 8(C2). To confirm this scenario, we have performed the GSO-B3LYP computation. The calculated spin densities are plotted in Fig. 9, being consistent with our conjecture. At long enough distances, the CHB energy provides the energy $(J_{\sigma_1\sigma_2} + J_{\pi_1\pi_2}) \cos \theta$ for the angle between spins of two oxygen atoms, θ . We note that

the intra-atomic (Hund coupling) terms, $-\sum_i^{1,2} J_{\sigma_i\pi_i}$ are strong enough to form the triplet oxygen atoms, so that we omitted these terms. Usually, $J_{\sigma_1\sigma_2} < J_{\pi_1\pi_2}$ holds, resulting in the singlet coupling of two oxygen atoms. It is noteworthy that this implies the spin-inversion, which can be directly applied for the singlet–triplet crossing reaction.⁸⁴ Thus, in the context of GSO-DFT approaches, there is no division between a spin-intermediate state and a spin-inversion process, for which the GSO solutions break the spin-symmetry concerning \hat{S}_z .

One might argue that most of the chemical properties such as a equilibrium distance and binding energies calculated by GSO-DFT are the same as those of usual ones, because the GSO solutions reduce to UKS ones at equilibrium and to sepa-

rated states in almost all cases. However, as an electronic structure approach to interconnect with molecular dynamics, the GSO treatment is obviously essential to describe chemical reactions when the oxygen type of the bond-dissociation is involved. Indeed, if we estimate the binding energy of the oxygen molecule by seeing the triplet potential surface of the usual UB3LYP computation with a 6-31G** basis, it becomes 189.32 kcal/mol, which is much larger than the experimental value, 118 kcal/mol. By utilizing the GSO-B3LYP/6-31G** method, the binding energy reduces to 124.54 kcal/mol, which is close to the experimental one.

Further, the spin intermediate states are often seen in the functional materials such as the single-molecular-magnet.⁸⁵ Thus, unfamiliar spin structures presented in this section, are needed as a guideline to control the reactivity or functionality of molecular compounds, because they have a more flexible magnetic structure than the traditional collinear magnetism.

Resonating KS-DFT as a Post GSO-DFT Approach

As emphasized in the preceding sections, the GSO-DFT is a very promising method for molecular magnetic systems. The near degenerate effects are treated via a broken-symmetry picture of GSO-DFT solutions. The line-up of broken pictures covers the almost all electronic structures such as 1D-, 2D-, and 3D-SDW, CDW, or CCW etc. However, there might be a serious problem in the case in which some of the above electronic structures coexist, such as the ionic radical systems. A very simple example beyond the broken-symmetry DFT is H_2^+ , as pointed out by Savin.⁵⁷ Even if we apply the GSO-DFT for ionic radicals, only one configuration can be described. For instance, only one configuration among the VB states in ionic radical state shown in Fig. 3 can be described well by a GSO picture, missing the resonance between these states. On the other hand, the CAS-based approach covers the all quantum fluctuations by including the configurations for the active electrons and the active orbitals that contribute to the resonating picture.^{33,34} However the CAS computation required the huge computational resources, as described above.

Thus, a remedy for these problems is the resonance of GSO configurations in a similar manner to that of the resonating Hartree–Fock (res HF) developed by Fukutome.⁸⁶ Compared to CAS-based approaches, the surpassing points of a res HF-type of the WFT approach are (i) that we exploited the electron correlation covered by broken-symmetry KS-DFT to reduce the number of expansion terms, and (ii) that we do not miss the physical picture of GSO solutions described in previous sections. The simple scheme of KS-DFT is several GSO-DFT computations to obtain different types of solutions, followed by the CI or multiconfiguration SCF (MCSCF) computation of ab initio Hamiltonian using those GSO-DFT solutions as a basis. This scheme is a particular kind of non-orthogonal CI or MCSCF. If we can find an appropriate generator coordinate (GC), μ , which is directly related to the types of GSO-solution, the resonating KS-DFT solution can be expanded as

$$|\Psi^{\text{Res-KS}}\rangle = \int d\mu |\mu\rangle \langle \mu | \Psi^{\text{Res-KS}} \rangle \quad (45)$$

$$\cong \sum_i \sum_{i_n} |\Phi_{(i,i_n)}^{\text{GSO-DFT}}\rangle \langle \Phi_{(i,i_n)}^{\text{GSO-DFT}} | \Psi^{\text{Res-KS}} \rangle.$$

Here i is an index for types of GSO solutions listed in Fig. 1. A sub-index, i_n refers to a distinct number of type-“ i ” solutions for the case that plural type-“ i ” solutions exist. In the actual computations of res HF of a Hubbard model⁸⁷ and a semi-empirical MO,⁸⁸ Igawa et al. showed that the results on spin-correlation function similar to the exact result for an 1D half-filled system, and on weights of components similar to the high-quality CI results for a carbon oxide, can be reproduced by the res HF. In both examples, they utilized a UHF-type solution, but introducing a GSO-type basis will spread the scope of this approach, for instance, for ubiquitous mixed valence multicenter transition-metal systems,⁸⁰ in which charge and 3D-canting-spins might coexist, required a superposition of CDW and TSW configurations of GSO-DFT to describe its electron structure. As an ab initio multiconfiguration (MC) approach to describe the electron correlation, Tomita et al. showed that the res HF with few MC’s covers a correlation energy of a carbon oxide to the same extent as CASSCF with a few hundred MC’s.⁸⁹ Very recently, Capelle⁹⁰ has applied a GC method by taking the parameter α of the X_α functional as a GC parameter, but without using broken symmetry features of KS solutions, for helium isoelectronic ions, yielding the nearly exact energies. If we will exploit the GSO picture of DFT, the resonating KS-DFT will be a powerful ab initio approach for both qualitative and quantitative purposes.

Regional Symmetry and Regional GSO-QM Approach for Macromolecular Systems

In the heterogeneous macromolecules such as metallo-enzymes⁹¹ involving the inorganic and organic building blocks, the electronic structures are different each other. For instance, the spin densities are usually more-or-less localized on the molecular units, including spin sources. Therefore it is enough to treat only regions neighboring the spin sources by the GSO-DFT, the remaining regions can be treated by the restricted DFT. And, for the case of an electron transfer reaction (ETR), the charge current flows along the path between the donor and acceptor sites.⁹² Thus, in order to describe an ETR in huge macromolecules, it is enough to set up the freedom of the charge current only on the electron-transfer path. The idea described here, in which we exploit only the essential degree of freedom in order to treat the macromolecular systems, is based on the classification of the current and spin-current KS-DFT solutions. The KS noninteracting energy to express this idea is given by

$$E_s \cong \min_{\mathbf{R}_{\text{TSW}}(\mathbf{r}) \rightarrow N} \left\{ T_s[\mathbf{R}_{\text{TSW}}(\mathbf{r})] + \sum_i \sum_{i_n} \int^{i_n} d\mathbf{r} \text{Tr} V_{\text{eff}}(\mathbf{r}) \mathbf{R}_i(\mathbf{r}) \right\}, \quad (46)$$

where the double-summation over i and i_n is same as that of the resonating KS equation given by Eq. 45. We here note that the integral region is divided into $\{\int^{i_n} d\mathbf{r}\}$ and $\mathbf{R}_i(\mathbf{r})$ is an effective fundamental variable for the region, $\int^{i_n} d\mathbf{r}$. Then, $\mathbf{R}_{\text{TSW}}(\mathbf{r})$ reduces to $\mathbf{R}_i(\mathbf{r})$ in this region. The kinetic term is expressed by KS orbitals as in the case of GSO-DFT. Some typical QM regions, of which the energy functional is given by

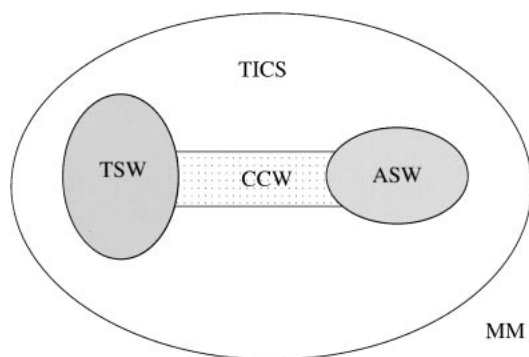


Fig. 10. A schematic representation of a partitioned system by the regional GSO-QM/MM approach. The TICS, ASDW, TSW, and CCW regions are treated by using the corresponding degree of freedom listed in Fig. 1.

$$E_s \cong \min_{R_{TSW}(\mathbf{r}) \rightarrow N} \left\{ T_s + \int^{TICS} d\mathbf{r} Tr V_{eff}(\mathbf{r}) R_{TICS}(\mathbf{r}) + \int^{TSW} d\mathbf{r} Tr V_{eff}(\mathbf{r}) R_{TSW}(\mathbf{r}) + \int^{ASDW} d\mathbf{r} Tr V_{eff}(\mathbf{r}) R_{ASW}(\mathbf{r}) + \int^{CCW} d\mathbf{r} Tr V_{eff}(\mathbf{r}) R_{CCW}(\mathbf{r}) \right\}, \quad (47)$$

are schematically illustrated in Fig. 10. The usual electronic structure of regions is the symmetry-restricted TICS one, spreading out like the sea. The active sites involving ASW and TSW states are expected to localize like islands. The temporal ETR path described by a CCW state bridges between these islands; the width of the path is determined by molecular species and environments. We call this scheme “the regional GSO-QM approach”.

Since the search region is directly related to the symmetry-framework, as shown in Fig. 5, we mean by Eq. 46 that we have introduced “the regional symmetry” to mask the degree of freedom of the first-order reduced density matrix. The ideas that the computational target is partitioned into many molecular units³⁷ and that, different electronic structure theories are applied for multi-layered regions,^{93,94} are already implemented successfully. Compared to those approaches, there are some different and superior points in our approach. First, our approach is based on the physical classification of GSO solutions so that the criterion for decomposition of the system is very clear. Second, if we appropriately divide the system into many regions, there are no points yielding discontinuities of physical properties, since the unnecessary freedom of $R_{TSW}(\mathbf{r})$ usually reduces. In addition, we adapt the same electronic structure theory except for the variable parameters for all regions, which is critically in contrast to ONIOM⁹³ and a semi-empirical + DFT approach,⁹⁴ so that there is no theoretical inconsistency concerning the level of the electronic correlation. The extension to regional GSO-QM/MM approach is straightforward. In that case, the outer region in Fig. 10 is treated by MM. The implementation of regional GSO-QM and regional GSO-QM/MM approaches will be presented elsewhere.

The Extended DFT for Quantum Electrodynamics

So far, our theoretical approaches are based on the broken-symmetry DFT within the nonrelativistic ab initio Hamiltonian. However, as described above, the GSO treatment of DFT enable us to describe the spin-inversion chemical reaction, which applies to spin-orbit interactions in the actual systems. Further, the 3D spin-structure of tetrahedral clusters presented by us follows symmetry operations that operate on both spin-and-spatial spaces simultaneously and that commute with spin-orbit term.⁵⁹ The most comprehensive group theory within $P \times S \times T$ for broken-symmetry GSO approaches based on first-order reduced density matrix is not a double-group or a magnetic group,⁵⁹ but a generalized magnetic double group derived by Ozaki and Fukutome.²⁵ Their theory can be applied for the GSO-DFT with spin-orbit corrections. However, if we take four-component of spinors into account, there are more extended treatments.

One of the recent topics in the electronic structure theory is the heavy fermion systems, in which both of the strong electron correlation and the relativistic effects of f electrons affect the electronic structures.⁹⁵ Many compounds of this class exhibit the spin-fluctuation-induced superconductivity.^{95–97} In particular, the recently discovered superconductors, $U\text{Pt}_3$ ⁹⁶ and Sr_2RuO_4 ,⁹⁷ have attracted great attentions in relation to those features, the odd-parity and the broken time-reversal symmetry, respectively. Previously, Ohsaku et al.⁹⁸ discussed the many-body electron correlation theories such as QED-SCF and QED-DMFT based on quantum electron dynamics (QED). They analyzed the 4×4 first order reduced density matrix from the viewpoint of symmetry including the time-reversal, parity, charge-conjugation. They also discuss the relation between relativistic DFT and nonrelativistic DFT. We touch their QED-DFT in the context of the extended DFT.

The fundamental variable of QED-DFT is the 4×4 density matrix expanded by using γ matrices with the Einstein notation as,

$$Q(\mathbf{r}S_1; \mathbf{r}S_2)(\equiv Q(\mathbf{X})) = Q_S(\mathbf{r})\mathbf{E} + Q_\mu^V(\mathbf{r})\gamma^\mu + Q_{\mu\nu}^T(\mathbf{r})\sigma^{\mu\nu} + Q_\mu^A(\mathbf{r})\gamma_5\gamma^\mu + Q^P(\mathbf{r})i\gamma_5, \quad (48)$$

where Q_S , Q_μ^V , $Q_{\mu\nu}^T$, and Q_μ^A are the scalar (S), the vector (V), 2-rank antisymmetric tensor (T), axial vector (A), and the pseudo-scalar (P) elements of Q , respectively. Here, \mathbf{E} and $\{\gamma^\mu\}_{\mu=0-3}$ are unit vector and Dirac gamma matrices as usual. Further, $\sigma^{\mu\nu} \equiv \frac{1}{2}[\gamma^\mu, \gamma^\nu]$ and $\gamma_5 \equiv i\gamma^0\gamma^1\gamma^2\gamma^3$. Q includes the four-current $\{j^\mu(\mathbf{r}) \equiv -e\langle\psi(\mathbf{r})\gamma^\mu\bar{\psi}(\mathbf{r})\rangle\}_{\mu=0-3}$, which coupled with external field $\{A_\mu^{\text{ext}}(\mathbf{r})\}_{\mu=0-3}$. Here $\psi(\mathbf{r})$ and $\bar{\psi}(\mathbf{r})$ are the Dirac field, and its Dirac conjugation, respectively. The QED version of the KS minimization is given by

$$E_s \cong \min_{Q(\mathbf{r})} \left\{ T_s + \int d\mathbf{r} j^\mu(\mathbf{r}) A_\mu^{\text{ext}}(\mathbf{r}) + E_{\text{XC}}[Q(\mathbf{r})] \right\}, \quad (49)$$

under constraint of conservation of the current and the total charge:

$$\partial_\mu j^\mu(\mathbf{r}) = 0, \quad \int d\mathbf{r} j_0(\mathbf{r}) = \text{constant}. \quad (50)$$

It is noteworthy that the XC term depends on the full compo-

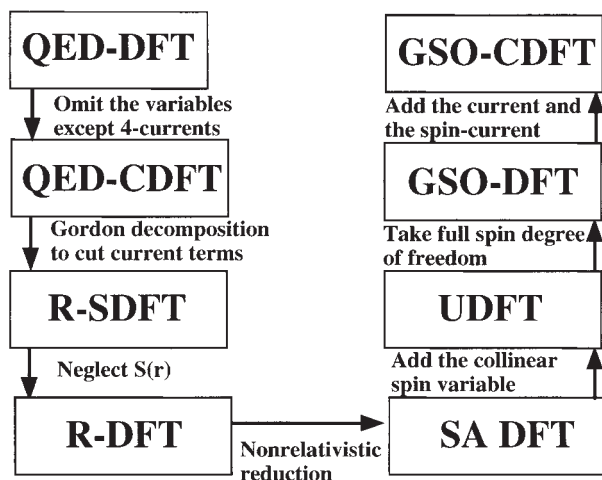


Fig. 11. The relation between several QED-DFTs and nonrelativistic broken-symmetry and symmetry-allowed DFTs.

nents of Q , so that the effective exchange potential for the KS equation also includes 16 elements corresponding the expansion of Eq. 48.

On the other hand, the usual treatment of QED current DFT (QED-CDFT)⁹⁹ is not for $Q(\mathbf{r})$, but for four-current, $j^\mu(\mathbf{r})$ as,

$$E_s \cong \min_{j^\mu(\mathbf{r})} \left\{ T_s + \int d\mathbf{r} j^\mu(\mathbf{r}) A_\mu^{\text{ext}}(\mathbf{r}) + E_{\text{XC}}[j^\mu(\mathbf{r})] \right\}. \quad (51)$$

The Gordon decomposition of $j(\mathbf{r}) = \mathbf{I}(\mathbf{r}) + \frac{\nabla \times \mathbf{S}(\mathbf{r})}{m}$ to cut the charge current components $\mathbf{I}(\mathbf{r}) \equiv \frac{i}{2m}(\psi \nabla \psi - (\nabla \psi) \psi)(\mathbf{r})$ leads to the relativistic spin DFT (RSDFT).¹⁰⁰ Further, we obtain the usual relativistic DFT by neglecting the vector components. The non-relativistic reduction to take only the large component of the 4-component spinor into account leads to non-relativistic symmetry-adapted KS-DFT. The generalization starting from SA KS-DFT to current-and-spin current KS-DFT is described the above sections. The schematic relations are illustrated in Fig. 11.

Development of the GSO-X Program

In the context of our theory, we have developed the ab initio program, which we called 'GSO-X', in the Biogrid project,¹⁰¹ which is a part of IT-program of Ministry of Education, Culture, Sports, Science and Technology. That program is constructed as the parallel version of a LCGTO program based on GSO. In addition, the symmetry-adapted (SA) version of GSO-X is developed to connect with the new version of AMOSS¹⁰² via the MPI-2 process-spawning technique.^{9,10} Further, these QM programs are connected to prestoX-basic for MM calculations, integrating to the platform towards biosimulation working simultaneously on heterogeneous computers by Nakamura and co-workers, which is referred as "BioPfuga".¹⁰³ The schematic illustration of BioPfuga is shown in Fig. 12. This platform is the first implementation of QM/MM applications going in the direction of the grid computation.¹⁰ The most remarkable feature of 'GSO-X' is, as described above, its potential to treat noncollinear molecular magnetism of tetrahedral clusters such as Fe_4S_4 and Mn_4O_4 , along with treating spin-canting or spin-inversion reactions involving oxygen mole-

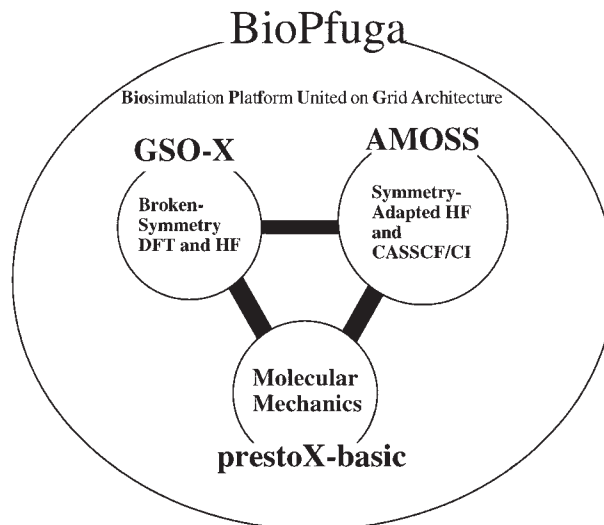


Fig. 12. The schematic illustration of the Biosimulation Platform United on Grid Architecture.

cules. Although these molecular units and reactions will be essential to describe the bioenzyme reactivities, there is no GSO version of an ab initio program among widely used ones like Gaussian 03¹⁰⁴ or GAMESS.¹⁰⁵ Therefore, by incorporating the merit of our GSO-DFT fully into this grid-computing oriented QM/MM, the new field of computational biochemistry based on ab initio approach is expected to be opened up.

Summary

We have discussed the extended DFT for the material design, in particular of molecular magnetism,² from the beginning of its theoretical backgrounds. Our approach is based on the pioneering work by precursors^{15–28} to cultivate the positive features of the broken-symmetry HF theory. Thus, we first reviewed their work. The classifications of solutions from the viewpoint of broken-symmetry patterns^{24–27} are excellent guidelines to investigate the electron structures of the strongly correlated systems. Further, the spin-unrestricted or GSO versions of HF theory cover part of nondynamical correlation via the spin densities of those solutions.²⁸ Both of these theories are directly related to the broken-symmetry KS-DFT.^{29,58,60–62}

We presented that the exact density of hydrogen molecule within the STO-3G is never obtained by any symmetry-adapted KS-DFT, while the broken-symmetry DFT provides the good approximation for the exact results, in particular for the strongly correlated region. This indicates that, to reproduce the exact densities, which are usually FON in the finite dimensional basis, we should employ the spin-unrestricted or GSO-DFT.⁵¹

Further, the relation between broken-symmetry patterns of GSO and constrained search regions of DFT is discussed in a manner similar to the classification of GHF solutions. We presented some examples for which the GSO treatment is essential. Our ab initio GSO-DFT approach^{58,67,68,70–72,74–76} is the first implementation in line with these stories, which are successfully applied for 3D spin-structures of multicenter metal systems, and the spin-canting reaction of oxygen-type cleavages. These computational results will be a first introduction of the molecular design by ab initio GSO approaches utilizing the full degree of freedom of the spins-and-orbitals.

In this paper, we also gave the weight to the future prospects of our approaches. The extensions to resonating KS-DFT, regional GSO-QM/MM, and QED-DFT are related to those of constrained search regions described for the GSO-DFT. Therefore, these are included in the extended DFT. The resonating KS-DFT allowing a superposition of several GSO configurations will be effective for the system in which various collective modes such as SDWs and CDW coexist, because the resonation among several states is beyond the theoretical scope of the GSO-DFT. We introduce the chemical-and-physical pictures into ab initio molecular dynamics by suggesting the regional QM/MM approach, in which huge systems are partitioned into many functional units having local chemical-and-physical characters. The QED-DFT as a most comprehensive theoretical framework of the extended DFT, enables us to treat the heavy fermions. This direction is expected to be a new ground for material science, since, compared with the usual GSO-DFT, there are more degrees of freedom to be broken in the fully four-component relativistic framework as described above.

The extended DFT approaches cover all of the magnetism, conductivities with-and-without spin-degree of freedom, as well as further quantum fluctuations, ab initio molecular dynamics and relativistic effects. We expect that these systematic approaches can provide not only qualitatively but also quantitatively excellent ab initio methods for molecular material design.

This work has been supported by a Grant-in-Aid for IT-program from Ministry of Education, Culture, Sports, Science and Technology. One of authors (S. Y.) acknowledges Dr. H. Nagao, Dr. M. Nakano, Dr. T. Oda, Prof. Y. Yoshioka, Prof. N. Suzuki, and all members of the Quantum Chemistry Laboratories of the Hokkaido University in 1992 and of the Osaka University in 1992–2003 for their helpful and valuable discussions.

References

- 1 K. Yoshida, "Theory of Magnetism," Springer (1996).
- 2 "Molecular Magnetism," ed by K. Itoh and M. Kinoshita, Gordon and Breach Science Publishers (2000); M. Tamura, Y. Nakazawa, D. Shiomi, K. Nozawa, Y. Hosokoshi, M. Ishikawa, M. Takahashi, and M. Kinoshita, *Chem. Phys. Lett.*, **186**, 401 (1991).
- 3 L. B. Coleman, M. J. Cohen, D. J. Sandman, F. F. Yamagishi, A. F. Garito, and A. J. Heeger, *Solid State Commun.*, **12**, 1125 (1973).
- 4 D. Jerome, A. Mazaud, M. Ribault, and K. Bechgaard, *J. Phys., Lett.*, **41**, L95 (1980).
- 5 "Quantum Chemistry," ed by K. Fukui, Asakura shoten, (in Japanese) (1968).
- 6 "Modern Quantum Chemistry," A. Szabo and N. S. Ostlund, Macmillan Publishing (1982); "Methods of Molecular Quantum Mechanics, Second Edition," M. Mcweeny, Academic Press (1992); "Quantum Mechanics in Chemistry," J. Simons and J. Nichols, Oxford University Press (1997); J. A. Pople, *Rev. Mod. Phys.*, **71**, 1267 (1999).
- 7 "Density Functional Theory of Atoms and Molecules," R. G. Parr and W. Yang, Oxford University Press (1989); W. Kohn, *Rev. Mod. Phys.*, **71**, 1253 (1999).
- 8 "How to Build a Beowulf—A Guide to the Implementation and Application of PC Clusters," T. L. Sterling, J. Salmon, D. J. Becker, and D. F. Savarese, MIT Press (1999).
- 9 "Parallel Programming with MPI," P. S. Pacheco, Morgan Kaufmann Publishers (1997); "Using MPI-2," W. Gropp, E. Lusk, and R. Thakur, MIT Press (1999).
- 10 "Grid Computing: Making the Global Infrastructure a Reality," F. Berman, G. Fox, T. Hey, and A. J. G. Hey, John Wiley & Sons (2003).
- 11 S. Goedecker, *Rev. Mod. Phys.*, **71**, 1085 (1999).
- 12 The special issue of QM/MM, *J. Mol. Struct.: THEOCHEM*, **632**, 1 (2003).
- 13 H. Nagao, M. Nakano, S. Yamanaka, Y. Shigeta, S. Yamada, D. Yamaki, I. Shigemoto, S. Kiribayashi, and K. Yamaguchi, *Int. J. Quantum Chem.*, **60**, 79 (1996).
- 14 C. C. J. Roothaan, *Rev. Mod. Phys.*, **23**, 61 (1951).
- 15 K. Yamaguchi, "Self-Consistent Field Theory and Applications," ed by R. Carbo and M. Klobukowski, Elsevier, Amsterdam (1990), p. 727.
- 16 P. O. Löwdin, *Rev. Mod. Phys.*, **35**, 496 (1963).
- 17 J. C. Slater, *Phys. Rev.*, **82**, 538 (1951).
- 18 K. Yamaguchi, T. Fueno, and H. Fukutome, *Chem. Phys. Lett.*, **22**, 461 (1973).
- 19 K. Yamaguchi, *Chem. Phys. Lett.*, **33**, 330 (1975).
- 20 K. Yamaguchi, *Chem. Phys. Lett.*, **35**, 230 (1975).
- 21 K. Yamaguchi and T. Fueno, *Chem. Phys. Lett.*, **38**, 47 (1976).
- 22 K. Yamaguchi and H. Fukutome, *Prog. Theor. Phys.*, **54**, 1599 (1975).
- 23 K. Yamaguchi and T. Fueno, *Chem. Phys. Lett.*, **38**, 52 (1976).
- 24 H. Fukutome, *Prog. Theor. Phys.*, **52**, 115 (1974).
- 25 M. Ozaki and H. Fukutome, *Prog. Theor. Phys.*, **60**, 1322 (1978).
- 26 M. Ozaki, *J. Math. Phys.*, **26**, 1514 (1985); *J. Math. Phys.*, **26**, 1521 (1985).
- 27 K. Yamaguchi, Y. Yabushita, and T. Fueno, *Chem. Phys. Lett.*, **46**, 360 (1977).
- 28 K. Yamaguchi, *Chem. Phys.*, **29**, 117 (1978).
- 29 J. P. Perdew, A. Savin, and K. Burke, *Phys. Rev. A*, **51**, 4531 (1995); J. P. Perdew, M. Ernzerhof, K. Burke, and A. Savin, *Int. J. Quantum Chem.*, **61**, 197 (1997).
- 30 B. Roos, B. R. Taylor, and P. E. M. Siegbahn, *Chem. Phys.*, **48**, 157 (1980).
- 31 K. Yamaguchi, K. Ohta, S. Yabushita, and T. Fueno, *Chem. Phys. Lett.*, **49**, 555 (1977).
- 32 S. Yamanaka, M. Okumura, M. Nakano, and K. Yamaguchi, *J. Mol. Struct.: THEOCHEM*, **310**, 205 (1994).
- 33 S. Yamanaka, M. Okumura, K. Yamaguchi, and K. Hirao, *Chem. Phys. Lett.*, **225**, 213 (1994).
- 34 S. Yamanaka, M. Okumura, H. Nagao, and K. Yamaguchi, *Chem. Phys. Lett.*, **233**, 88 (1995).
- 35 S. Yamanaka, T. Kawakami, M. Okumura, and K. Yamaguchi, *Chem. Phys. Lett.*, **233**, 257 (1995).
- 36 K. Hirao, *Chem. Phys. Lett.*, **190**, 397 (1992); K. Anderson, P. A. Malmqvist, and B. O. Roos, *J. Chem. Phys.*, **96**, 1218 (1992).
- 37 K. Kitaura, E. Ikeo, T. Asada, T. Nakano, and M. Uebayashi, *Chem. Phys. Lett.*, **313**, 701 (1999); T. Nakano, T. Kaminuma, T. Sato, T. Akiyama, M. Uebayashi, and K. Kitaura, *Chem. Phys. Lett.*, **318**, 614 (2000); Y. Komeji, T. Nakano, K. Fukazawa, Y. Ueno, Y. Inadomi, T. Nemoto, M. Uebayashi, D. G. Fedorov, and K. Kitaura, *Chem. Phys. Lett.*, **372**, 342 (2003).

- 38 A. Caneschi, D. Gatteschi, C. Sangregorio, R. Sessoli, L. Sorace, A. Cornia, M. A. Novak, C. Pulsen, and W. Wernsdorfer, *J. Magn. Magn. Mater.*, **200**, 182 (1999).
- 39 U. von Barth and L. Hedin, *J. Phys. C: Solid State Phys.*, **5**, 1629 (1972).
- 40 A. Görling, *Phys. Rev. A*, **47**, 2783 (1993).
- 41 M. M. Pant and A. K. Rajagopal, *Solid State Commun.*, **10**, 1157 (1972).
- 42 W. Koch and M. C. Hothausen, "A Chemist's Guide to Density Functional Theory," Wiley-VCH (2001).
- 43 P. Hohenberg and W. Kohn, *Phys. Rev. B*, **136**, 864 (1964); M. Levy, *Proc. Natl. Acad. Sci. U.S.A.*, **76**, 6062 (1979).
- 44 S. H. Vosko, L. Wilk, and M. Nusair, *Can. J. Phys.*, **58**, 1200 (1980).
- 45 A. Becke, *Phys. Rev. A*, **38**, 3098 (1988); C. Lee, W. Yang, and R. G. Parr, *Phys. Rev. B*, **37**, 785 (1988).
- 46 J. P. Perdew, J. A. Chevary, S. H. Vosko, S. A. Jackson, M. R. Pederson, D. J. Singh, and C. Fiolhais, *Phys. Rev. B*, **46**, 6671 (1992); J. P. Perdew, K. Burke, and M. Ernzerhof, *Phys. Rev. Lett.*, **77**, 3865 (1996).
- 47 S. Kurth, J. P. Perdew, and P. Blaha, *Int. J. Quantum Chem.*, **75**, 899 (1999).
- 48 A. Becke, *J. Chem. Phys.*, **98**, 5648 (1993).
- 49 B. I. Dunlap, "Density Functional Methods in Chemistry," Springer-Verlag (1991).
- 50 M. Filatov and S. Shaik, *Chem. Phys. Lett.*, **304**, 429 (1999).
- 51 R. Takeda, S. Yamanaka, and K. Yamaguchi, *Int. J. Quantum Chem.*, **93**, 313 (2003).
- 52 B. Miehlich, H. Stoll, and A. Savin, *Mol. Phys.*, **91**, 527 (1997); J. Grafenstein and D. Cremer, *Chem. Phys. Lett.*, **316**, 569 (2000).
- 53 R. Takeda, S. Yamanaka, and K. Yamaguchi, *Chem. Phys. Lett.*, **366**, 321 (2002).
- 54 P. Pollet, A. Savin, T. Leininger, and H. Stoll, *J. Chem. Phys.*, **116**, 1250 (2002); E. San-Fabián and N. L. Pastor-Abia, *Int. J. Quantum Chem.*, **91**, 451 (2003).
- 55 U. von Barth, *Phys. Rev. A*, **20**, 1693 (1979).
- 56 M. Levy and J. P. Perdew, "Density Functional Methods in Physics," ed by R. M. Dreizler and J. da Providencia, Plenum, New York (1985).
- 57 A. Savin, "Recent Developments and Applications of Modern Density Functional Theory," ed by J. M. Seminario, Elsevier (1996).
- 58 S. Yamanaka, T. Kawakami, H. Nagao, and K. Yamaguchi, *Chem. Phys. Lett.*, **231**, 25 (1994); S. Yamanaka, T. Kawakami, S. Yamada, H. Nagao, M. Nakano, and K. Yamaguchi, *Chem. Phys. Lett.*, **240**, 268 (1995).
- 59 T. Inui, Y. Tanabe, and Y. Onodera, "Group Theory and Its Applications in Physics," Springer, Berlin (1990).
- 60 K. Yamaguchi, *Chem. Phys. Lett.*, **66**, 395 (1979).
- 61 B. Weiner and S. B. Trickey, *Int. J. Quantum Chem.*, **69**, 451 (1998).
- 62 S. Yamanaka, T. Ohsaku, D. Yamaki, and K. Yamaguchi, *Int. J. Quantum Chem.*, **91**, 376 (2003).
- 63 G. Vignale, M. Rasolt, and D. J. W. Geldart, *Adv. Quantum Chem.*, **21**, 235 (1990).
- 64 O. Gunnarsson and B. I. Lundqvist, *Phys. Rev. B*, **13**, 4274 (1976).
- 65 J. Kübler, "Theory of Itinerant Electron Magnetism," Clarendon Press, Oxford, UK (2000), and references therein.
- 66 T. Oda, A. Pasquarello, and R. Car, *Phys. Rev. Lett.*, **80**, 3622 (1998).
- 67 S. Yamanaka, D. Yamaki, Y. Shigeta, H. Nagao, Y. Yoshioka, N. Suzuki, and K. Yamaguchi, *Int. J. Quantum Chem.*, **80**, 664 (2000).
- 68 S. Yamanaka, D. Yamaki, Y. Shigeta, H. Nagao, and K. Yamaguchi, *Int. J. Quantum Chem.*, **84**, 670 (2001).
- 69 M. Körling and J. Ergon, *Phys. Rev. B*, **54**, R8293 (1996).
- 70 S. Yamanaka, D. Yamaki, S. Kiribayashi, and K. Yamaguchi, *Int. J. Quantum Chem.*, **85**, 421 (2001).
- 71 S. Yamanaka, Y. Shigeta, Y. Ohta, D. Yamaki, H. Nagao, and K. Yamaguchi, *Int. J. Quantum Chem.*, **84**, 369 (2001).
- 72 S. Yamanaka, R. Takeda, and K. Yamaguchi, *Polyhedron*, **22**, 2013 (2003).
- 73 A. Yoshimori, *J. Phys. Soc. Jpn.*, **14**, 807 (1959).
- 74 S. Yamanaka, R. Takeda, and K. Yamaguchi, *Mol. Cryst. Liq. Cryst.*, **379**, 537 (2002).
- 75 S. Yamanaka, R. Takeda, T. Kawakami, S. Nakano, D. Yamaki, S. Yamada, K. Nakata, T. Sakuma, T. Takada, and K. Yamaguchi, *Int. J. Quantum Chem.*, **95**, 512 (2003).
- 76 S. Yamanaka, R. Takeda, T. Kawakami, K. Nakata, T. Sakuma, T. Takada, and K. Yamaguchi, *J. Magn. Magn. Mater.*, in press.
- 77 K. Yamaguchi, T. Fueno, M. Ozaki, N. Ueyama, and A. Nakamura, *Chem. Phys. Lett.*, **168**, 56 (1990).
- 78 H. Fukutome, M. Takahashi, and T. Takabe, *Prog. Theor. Phys.*, **53**, 1580 (1975).
- 79 K. Yamaguchi, *Chem. Phys. Lett.*, **30**, 288 (1975).
- 80 K. Yamaguchi, S. Yamanaka, M. Nishino, Y. Takano, Y. Kitagawa, H. Nagao, and Y. Yoshioka, *Theor. Chim. Acta.*, **102**, 328 (1999).
- 81 G. C. Papaefthymiou, E. J. Lasknowski, S. Frota-Pessoa, R. B. Frankel, and R. H. Holm, *Inorg. Chem.*, **21**, 1723 (1982).
- 82 J. Aussoleil, P. Cassoux, P. de Loth, and J. P. Tuchagues, *Inorg. Chem.*, **28**, 3051 (1989).
- 83 Y. Tokura and N. Nagaosa, *Science*, **288**, 462 (2000); T. Kawamoto and N. Suzuki, *J. Phys. Soc. Jpn.*, **66**, 2487 (1997).
- 84 M. C. Lin, "Potential Surfaces," ed by K. P. Lawle, John Wiley & Sons, New York (1980); D. Schröder, H. Schwarz, and S. Shaik, *Struct. Bonding*, **97**, 91 (2000); K. Yoshizawa, Y. Shiota, and T. Yamabe, *J. Am. Chem. Soc.*, **121**, 147 (1999); G. Zhang, S. Li, and Y. Jiang, *Organometallics*, **22**, 3820 (2003); S. Bärsch, D. Schröder, and H. Schwarz, *J. Phys. Chem. A*, **105**, 2005 (2001).
- 85 G. Christou, "Magnetism: A Supramolecular Function" ed by O. Kahn (1996), p. 383; S. L. Carsto, Z. Sun, C. M. Grant, J. C. Bollinger, D. N. Hendrickson, and G. Christou, *J. Am. Chem. Soc.*, **120**, 2365 (1998).
- 86 H. Fukutome, *Prog. Theor. Phys.*, **80**, 417 (1988).
- 87 A. Igawa, S. Yamamoto, and H. Fukutome, *J. Phys. Soc. Jpn.*, **62**, 1653 (1993).
- 88 A. Igawa and H. Fukutome, *Prog. Theor. Phys.*, **80**, 611 (1988).
- 89 N. Tomita, S. Ten-no, and Y. Tanimura, *Chem. Phys. Lett.*, **263**, 687 (1996).
- 90 K. Capelle, *J. Chem. Phys.*, **119**, 1286 (2003).
- 91 "Metal Clusters in Proteins," ed by L. Que, Jr., American Chemical Society (1988).
- 92 I. Daizaeh, J. Guo, and A. Stuchebrukhov, *J. Chem. Phys.*, **110**, 8865 (1999); J. Wang and A. A. Stuchebrukhov, *Int. J. Quantum Chem.*, **80**, 591 (2000); F. Guerlesquin, M. Bruschi, and G. Bovier-Lapierre, *Biochimie*, **66**, 93 (1984).
- 93 T. Vervan and K. Morokuma, *J. Comput. Chem.*, **21**, 1419 (2000).
- 94 Q. Cui, H. Guo, and M. Karplus, *J. Chem. Phys.*, **117**, 5617

(2002).

95 G. R. Stewart, *Rev. Mod. Phys.*, **56**, 755 (1984).

96 G. M. Luke, A. Keren, L. P. Le, W. D. Wu, Y. J. Uemura, D. A. Bonn, L. Taillefer, and J. D. Garrett, *Phys. Rev. Lett.*, **71**, 1466 (1993); R. Joynt and L. Taillefer, *Rev. Mod. Phys.*, **74**, 235 (2002).

97 G. M. Luke, Y. Fudamoto, K. M. Kojima, M. I. Larkin, J. Merrin, B. Nachumi, Y. J. Uemura, Y. Maeno, Z. Q. Mao, Y. Mori, H. Nakamura, and M. Sigrist, *Nature (London)*, **394**, 558 (1998); E. Dumont and A. Mota, *Phys. Rev. B*, **65**, 144519 (2003).

98 T. Ohsaku and K. Yamaguchi, *Int. J. Quantum Chem.*, **85**, 272 (2001); T. Ohsaku, S. Yamanaka, D. Yamaki, and K. Yamaguchi, *Int. J. Quantum Chem.*, **90**, 273 (2002).

99 E. Engel, "Relativistic Electronic Structure Theory, Part I, Fundamentals," ed by R. Schwerdtfeger, Elsevier (2002).

100 H. Eschrig and V. D. P. Servedio, *J. Comput. Chem.*, **20**, 23 (1999).

101 <http://www.biogrid.jp>

102 "SUPER-UX Molecular Orbital Calculation System AMOSS. Users Guide," NEC Corp., Tokyo, 1992.

103 H. Nakamura, S. Date, H. Matsuda, and S. Shimojo, *A Challenge New Gene. Comp.*, in press.

104 M. J. Frisch, G. W. Trucks, H. B. Schlegel, G. E. Scuseria,

M. A. Robb, J. R. Cheeseman, J. A. Montgomery, Jr., T. Vreven, K. N. Kudin, J. C. Burant, J. M. Millam, S. S. Iyengar, J. Tomasi, V. Barone, B. Mennucci, M. Cossi, G. Scalmani, N. Rega, G. A. Petersson, H. Nakatsuji, M. Hada, M. Ehara, K. Toyota, R. Fukuda, J. Hasegawa, M. Ishida, T. Nakajima, Y. Honda, O. Kitao, H. Nakai, M. Klene, X. Li, J. E. Knox, H. P. Hratchian, J. B. Cross, C. Adamo, J. Jaramillo, R. Gomperts, R. E. Stratmann, O. Yazyev, A. J. Austin, R. Cammi, C. Pomelli, J. W. Ochterski, P. Y. Ayala, K. Morokuma, G. A. Voth, P. Salvador, J. J. Dannenberg, V. G. Zakrzewski, S. Dapprich, A. D. Daniels, M. C. Strain, O. Farkas, D. K. Malick, A. D. Rabuck, K. Raghavachari, J. B. Foresman, J. V. Ortiz, Q. Cui, A. G. Baboul, S. Clifford, J. Cioslowski, B. B. Stefanov, G. Liu, A. Liashenko, P. Piskorz, I. Komaromi, R. L. Martin, D. J. Fox, T. Keith, M. A. Al-Laham, C. Y. Peng, A. Nanayakkara, M. Challacombe, P. M. W. Gill, B. Johnson, W. Chen, M. W. Wong, C. Gonzalez, and J. A. Pople, "Gaussian 03, Revision A.1," Gaussian, Inc., Pittsburgh PA (2003).

105 M. W. Schmidt, K. K. Baldridge, J. A. Boatz, S. T. Elbert, M. S. Gordon, J. H. Jensen, S. Koseki, N. Matsunaga, K. A. Nguyen, S. Su, T. L. Windus, M. Dupuis, and J. A. Montgomery, *J. Comput. Chem.*, **14**, 1347 (1993).



Shusuke Yamanaka was born in Amagasaki, Hyogo in 1969. He received his Ph. D. degree in 1999 from Osaka University. In 1999, he has been a research fellow of the Japan Society for the Promotion of Science. Starting October of 1999, he has been a research associate at the Graduate School of Science, Osaka University. In 2002, he was appointed as a postdoctoral researcher of the Biogrid project, which is a part of IT-program of the Japanese Ministry of Education, Culture, Sports, Science and Technology, on the development of ab initio QM/MM program towards grid-computing. His current research has focused on the development of generalized spin orbital density functional theory and its application to noncollinear molecular magnetism, as well as its extension to multi-reference approaches, QM/MM, and relativistic theories.